Study of Nail-soil Interaction by Numerical Shear Box Test Simulations

GEO Report No. 265

W.M. Cheung & G.W.K. Chang

Geotechnical Engineering Office
Civil Engineering and Development Department
The Government of the Hong Kong
Special Administrative Region

Study of Nail-soil Interaction by Numerical Shear Box Test Simulations

GEO Report No. 265

W.M. Cheung & G.W.K. Chang

This report was originally produced in February 2009 as GEO Special Project Report No. SPR 1/2009

First published, March 2012

Prepared by:

Geotechnical Engineering Office,
Civil Engineering and Development Department,
Civil Engineering and Development Building,
101 Princess Margaret Road,
Homantin, Kowloon,
Hong Kong.

Preface

In keeping with our policy of releasing information which may be of general interest to the geotechnical profession and the public, we make available selected internal reports in a series of publications termed the GEO Report series. The GEO Reports can be downloaded from the website of the Civil Engineering and Development Department (http://www.cedd.gov.hk) on the Internet. Printed copies are also available for some GEO Reports. For printed copies, a charge is made to cover the cost of printing.

The Geotechnical Engineering Office also produces documents specifically for publication in print. These include guidance documents and results of comprehensive reviews. They can also be downloaded from the above website.

The publications and the printed GEO Reports may be obtained from the Government's Information Services Department. Information on how to purchase these documents is given on the second last page of this report.

Y.C. Chan
Head, Geotechnical Engineering Office
March 2012

Foreword

This study forms a part of a series of nail-soil interaction studies. Numerical simulations of direct shear box and zone shear box tests have been carried out to examine the soil-interaction of soil nails in respect of lateral soil pressure, and the mobilisation of axial force, shear force and bending moment in the soil nails. The findings of the study lay out a framework for examining the feasibility of using new material other than steel for soil-nail reinforcement.

The study was carried out by Dr R.W.M. Cheung and Dr G.W.K. Chang of the Standards and Testing Division. Many other colleagues provided constructive comments on a draft of this report. Their contributions are gratefully acknowledged.

W.K. Pun
Chief Geotechnical Engineer/Standards & Testing

Abstract

Soil nailing has been commonly used as a structural support to enhance stability of existing and newly formed slopes. Its performance is generally satisfactory, however, the current design approach has made little account for the nail-ground interaction in particular if new materials other than steel are used for soil-nail reinforcement. A study using simulated direct shear box and zone shear box has been carried out to investigate the behaviour of steel soil-nail reinforcement subject to shearing with and without contrast in soil stiffness between the two shear zones.

The results indicate that axial force, shear force and bending moment were mobilised when the soil nail was subject to shearing. The distributions of axial force, shear force and bending moment generally resemble those determined theoretically. The degree of mobilisation increases as the width of shear zone decreases, and as the contrast in soil stiffness increases. Among the mobilisation of axial force, shear force and bending moment, the latter is the highest irrespective of the width of shear zone and the contrast in soil stiffness.

This report presents the details and findings of the study.

Contents

		Page No.
Title Page		1
Preface		3
Foreword		4
Abstract		5
Contents		6
List of Tables		7
List of Figures		8
1	Introduction	10
2	Effect of Shearing and Bending on Soil-nail Reinforcement	10
2.1	Past Experimental and Theoretical Studies	10
2.2	Numerical Simulations	12
2.2.1	General	12
2.2.2	Assumptions	12
2.2.3	Modelling of Shear Plane	15
2.2.3.1	Numerical Model - Direct Shear Box Test	15
2.2.3.2	Results and Discussions	15
2.2.4	Modelling of Shear Zone	20
2.2.4.1	Numerical Model - Zone Shear Box Test	20
2.2.4.2	Results and Discussions	26
2.2.5	Modelling of Ground with Contrast Stiffness	26
2.2.5.1	Results and Discussions	26
2.3	Technical Implications	41
3	Conclusions	41
4	References	42

List of Tables

Table No.		Page No.
2.1	Summary of Results on Numerical Direct Shear Box Test and Zone Shear Box Test Simulation	16
2.2	Summary of Results on Numerical Direct Shear Box Test Simulations with Soils of Contrast in Stiffness	27

List of Figures

Figure No.		Page No.
2.1	Distribution of (a) Bending Moment (M/M_p), (b) Shear Force (P_s/P_p) and (c) Lateral Stress (σ'_l/σ'_b) at a Shear Displacement of 60 mm (after Pedley, 1990)	11
2.2	Simplified Distributions of Net Lateral Soil Pressure on a Soil-nail for Different Failure Modes (Modified Tan et al, 2000)	13
2.3	Shear Patterns Generated by Different Types of Shear Box Test Simulations	14
2.4	Details of Numerical Direct Shear Box Test Simulation	17
2.5	Net Lateral Soil Pressure Distribution along the Soil Nail in Numerical Direct Shear Box Test Simulation	18
2.6	Distributions of Shear Force, Bending Moment and Axial Force along the Soil Nail in the Numerical Direct Shear Box Test Simulation When δ = 5 mm	21
2.7	Distributions of Shear Force, Bending Moment and Axial Force along the Soil Nail in the Numerical Direct Shear Box Test Simulation When δ = 10 mm	22
2.8	Distributions of Shear Force, Bending Moment and Axial Force along the Soil Nail in the Numerical Direct Shear Box Test Simulation When δ = 25 mm	23
2.9	Distributions of Shear Force, Bending Moment and Axial Force along the Soil Nail in the Numerical Direct Shear Box Test Simulation When δ = 50 mm	24
2.10	Details of Numerical Zone Shear Box Test Simulation	25
2.11	Net Lateral Soil Pressure Distribution along the Soil Nail in 100 mm Numerical Zone Shear Box Test Simulation	28
2.12	Net Lateral Soil Pressure Distribution along the Soil Nail in 200 mm Numerical Zone Shear Box Test Simulation	30
2.13	Distributions of Shear Force, Bending Moment and Axial Force along the Soil Nail in the 100 mm Zone Numerical Shear Box Test Simulation When δ = 5 mm	32

Figure No.		Page No.
2.14	Distributions of Shear Force, Bending Moment and Axial Force along the Soil Nail in the 100 mm Zone Numerical Shear Box Test Simulation When δ = 10 mm	33
2.15	Distributions of Shear Force, Bending Moment and Axial Force along the Soil Nail in the 100 mm Zone Numerical Shear Box Test Simulation When δ = 25 mm	34
2.16	Distributions of Shear Force, Bending Moment and Axial Force along the Soil Nail in the 100 mm Zone Numerical Shear Box Test Simulation When δ = 50 mm	35
2.17	Distributions of Shear Force, Bending Moment and Axial Force along the Soil Nail in the 200 mm Zone Numerical Shear Box Test Simulation When δ = 5 mm	36
2.18	Distributions of Shear Force, Bending Moment and Axial Force along the Soil Nail in the 200 mm Zone Numerical Shear Box Test Simulation When δ = 10 mm	37
2.19	Distributions of Shear Force, Bending Moment and Axial Force along the Soil Nail in the 200 mm Zone Numerical Shear Box Test Simulation When δ = 25 mm	38
2.20	Distributions of Shear Force, Bending Moment and Axial Force along the Soil Nail in the 200 mm Zone Numerical Shear Box Test Simulation When δ = 50 mm	39
2.21	Details of Numerical Direct Shear Box Test Simulation with Soils of Contrast in Stiffness	40

1 Introduction

The soil nailing technique was introduced to Hong Kong in the 1980s. Since the early 1990s, the technique has been popular in enhancing the stability of existing and newly formed slopes. Experience gained over the years of application has led to the publication of the Geoguide 7 : Guide to Soil Nail Design and Construction (GEO, 2008), which summarised the standard of good practice for the design, construction, monitoring and maintenance of soil-nailed systems.

As steel reinforcement has high shear ductility, which renders the failure mode of a soil-nailed system likely to be ductile, it is generally not necessary to check against bending and shear failure of steel reinforcement in design. With the advancement of material technology, the potential of using new materials as an alternative to steel bars for soil-nail reinforcement will increase. Among those factors listed in Geoguide 7, the susceptibility to bending or shear failure should be considered if an alternative material other than steel is used as soil-nail reinforcement.

Numerical modelling provides a tool to investigate the behaviour of a soil-nail reinforcement subject to shearing. In this study, the element behaviour of a soil-nail reinforcement under shearing was studied by means of numerical shear box test simulation using the finite element programme, PLAXIS (Version 8). The reinforcement was placed normal to the shear plane. This is to examine the behaviour of the reinforcement under the worst scenario in respect of maximum bending and shear force. The bending moments and forces obtained from the numerical simulations were also compared with theoretical values.

2 Effect of Shearing and Bending on Soil-nail Reinforcement

2.1 Past Experimental and Theoretical Studies

When a soil nail is being sheared, lateral soil pressures will be developed on both sides of the soil-nail reinforcement, and hence the development of axial force (tension or compression), bending moment and shear force. Figure 2.1 reproduces some experimental results showing the distributions of bending moment, shear force and lateral soil stress in shear box tests obtained by Pedley (1990). A key finding of his study is that the maximum moblised shear forces are well below their ultimate values even though the corresponding bending moments are close to their plastic values.

On the basis of the experimental and theoretical work by Pedley (1990) and Jewell & Pedley (1992), Tan et al (2000) proposed the following simplified failure modes to describe the nail-soil lateral interaction when a soil-nail reinforcement is subjected to shearing:

(a) Mode A1: Plastic soil-elastic nail failure mode.

(b) Mode A2: Plastic soil-plastic nail failure mode.

(c) Mode B: Plastic nail-elastic soil failure mode.

(d) Mode C: Plastic soil-nail failure mode.

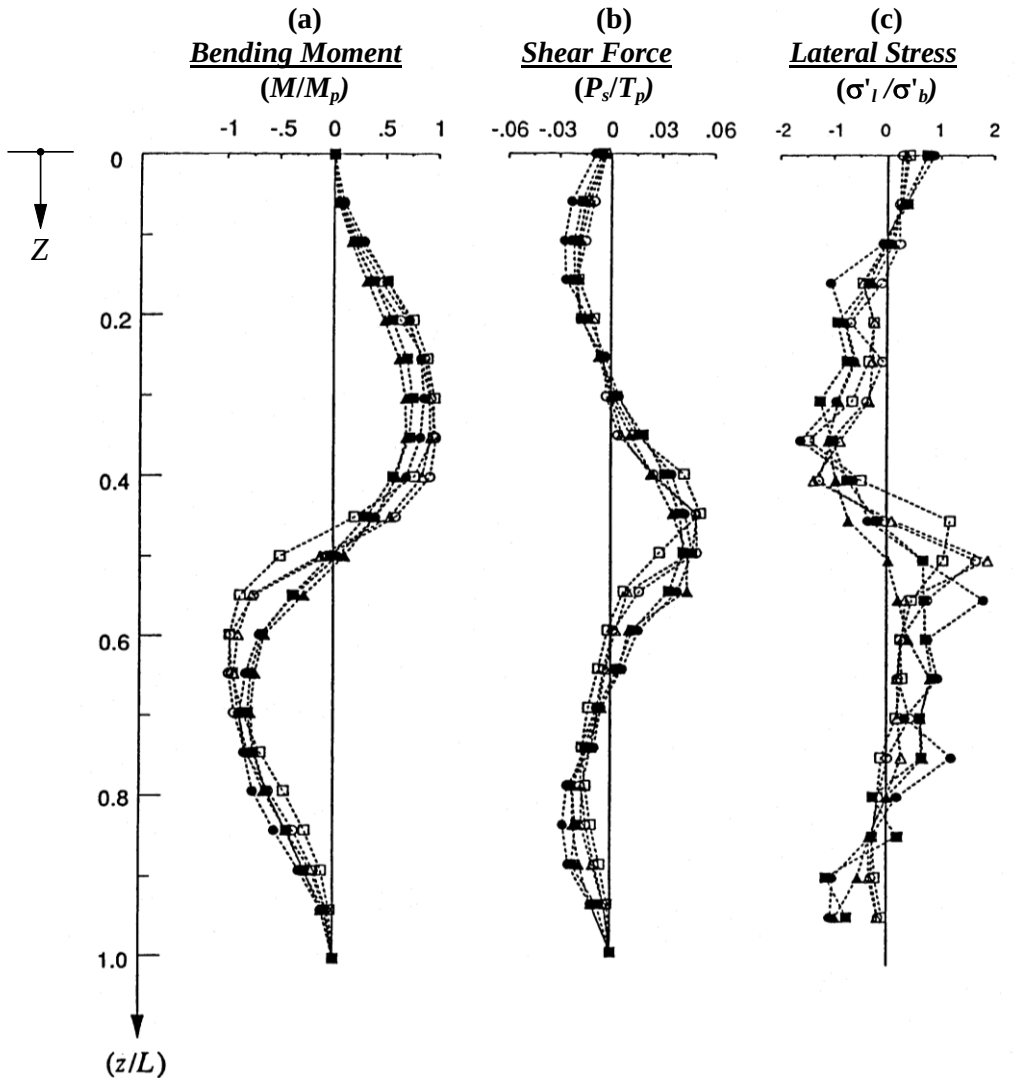

	Bar diameter (mm)	Nail orientation θ°		Bar diameter (mm)	Nail orientation θ°
○	15.88	0°	●	25.4	0°
□	15.88	15°	■	25.4	15°
△	15.88	25°	▲	25.4	25°

Legend:

M	Bending moment of nail	L	Total length of nail
M_P	Fully plastic bending moment of nail	z	Distance measured from origin in the Z direction
P_s	Nail shear force		
T_P	Fully plastic axial force in nail	θ	Angle made between nail and the normal to the shear plane
σ'_l	Lateral stress on nail		
σ'_b	Limiting bearing stress		

Note: The plastic shear force, $P_p \approx \frac{T_p}{2}$

Figure 2.1 Distribution of (a) Bending Moment (M/M_p), (b) Shear Force (P_s/P_p) and (c) Lateral Stress (σ'_l/σ'_b) at a Shear Displacement of 60 mm (after Pedley, 1990)

Mode A1 failure will occur if a soil nail is relatively stiffer and stronger than the surrounding soil. Mode A2 failure is a further development of Mode A1 when the relative displacement between the soil and soil nail increases. Mode B failure will occur if the soil is relatively stiffer and stronger than the soil nail, whereas Mode C failure will occur when the soil nail and the soil have compatible stiffness and they reach their plastic stages simultaneously. The distributions of net lateral soil pressure for failure modes A1, A2 and B are shown in Figure 2.2. Failure mode C is a special case of mode A1 and therefore has a similar distribution of lateral soil pressure as shown in Figure 2.2, except that the point of maximum bending moment is replaced by the point of moment capacity of the soil nail.

2.2 Numerical Simulations

2.2.1 General

The nail-soil interaction under direct shearing was investigated using numerical shear box test simulation with different boundary conditions. Figure 2.3 shows schematically the shear patterns generated by the two types of shear box test simulations. They are (a) the direct shear box test and (b) the zone shear box test. The direct shear box test simulation allows a designated failure plane to develop, whilst the zone shear box test simulates a designated uniform shearing zone across the nail.

Numerical shear box test simulations were conducted using the finite element computer programme PLAXIS. The following scenarios were considered in the numerical simulations:

(a) Shearing plane.

(b) Shearing zone with thickness of 100 mm and 200 mm.

(c) Contrast in soil stiffness between the two halves of the shear box.

2.2.2 Assumptions

A 25 mm diameter steel bar was modelled in the present study. The following assumptions were made in the numerical simulations:

(a) The effect of soil pressure re-distribution in the direction normal to the paper (z-direction) was ignored in the 2-dimensional (plane-strain) model.

(b) The results including the axial force, the shear force and the bending moment for a single steel bar were simply taken by dividing the results per metre run by the total equivalent number of bars in the 2-dimensional analysis, i.e. 40.

(c) The effect of reinforcement ribs on the nail-soil interaction was ignored.

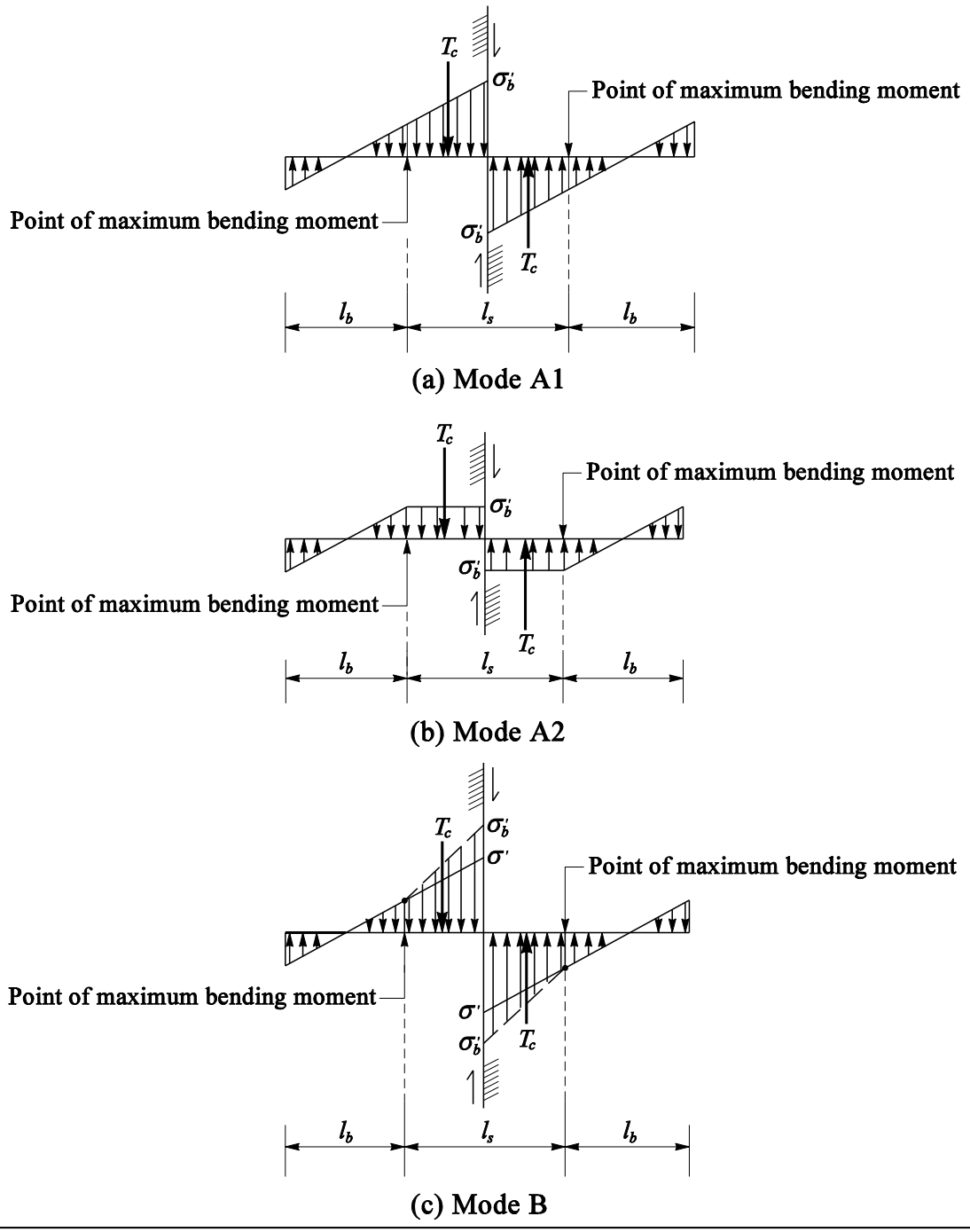

Legend:

σ_b'	Soil limit bearing pressure
σ'	Soil pressure on soil nail
T_c	Nail-soil lateral resistance
l_s	Width of shear band
l_b	The minimum soil-nail length required beyond the point of maximum bending moment

Figure 2.2 Simplified Distributions of Net Lateral Soil Pressure on a Soil-nail for Different Failure Modes (Modified Tan et al, 2000)

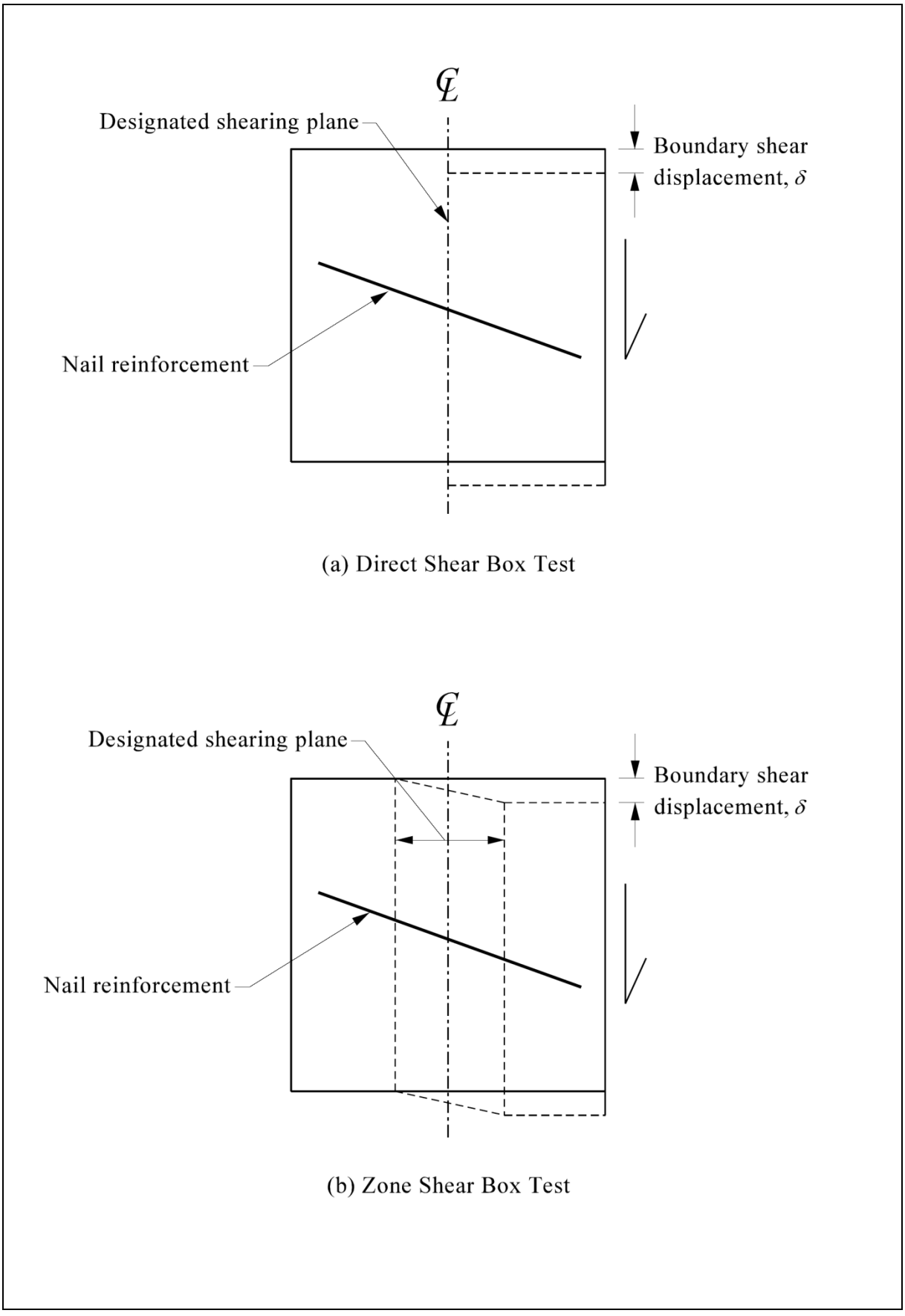

Figure 2.3 Shear Patterns Generated by Different Types of Shear Box Test Simulations

(d) Interface elements were used to model the interface between soil and the nail. The reduction factor in shear strength, R_{inter}, for the interface between the nail and the soil was taken as 0.66 in this comparative study as recommended by the PLAXIS.

(e) A Mohr-Coulomb elastic-perfectly-plastic model was employed.

(f) The effect of soil contraction/dilation during shearing was ignored.

2.2.3 Modelling of Shear Plane

2.2.3.1 Numerical Model - Direct Shear Box Test

The simulated shear box has dimensions of 1 m wide x 3 m deep and a length of 6 m split into two halves. A 1 m wide steel plate equivalent to 40 no. of 25 mm diameter and 3 m long steel bars was inserted in the middle of the box across the vertical slip surface. The box was filled with homogeneous sand. The details of the model shear box, and the soil and steel parameters are given in Figure 2.4.

A 2-dimensional (plane strain) Mohr-Coulomb model was used for the soil. The shear box was initially restrained to move horizontally at both the right-hand and the left-hand sides, and restrained to move vertically at the bottom. A pressure of 80 kN/m^2 was applied on the top of the box to model a 5 m high overburden pressure. An imposed uniform boundary shear displacement δ of 5 mm, 10 mm, 25 mm and 50 mm was then applied in sequence in the downward direction y along the top and bottom of the right half of the box, simulating the uniform downward movement of the right half of the shear box. The lateral soil bearing pressure would be generated as a function of the relative displacement between the soil and the plate, and the interaction between them was then investigated.

2.2.3.2 Results and Discussions

For each imposed boundary shear displacement δ, the net lateral soil pressures σ_l obtained from the numerical simulations are shown in Figure 2.5. The theoretical net lateral soil pressure distributions for failure modes A1 and A2 as described in Section 2.1 are also plotted in the figures for comparison.

The maximum shear force Ps_{max}, maximum bending moment M_{max} and maximum axial force T_{max} of nail reinforcement corresponding to boundary shear displacement δ of 5 mm, 10 mm, 25 mm and 50 mm, together with those for zone shear box test simulations (see Section 2.2.4) are shown in Table 2.1. The distributions of shear force, bending moment and axial force along the soil nail corresponding to boundary shear displacement δ of 5 mm, 10 mm, 25 mm and 50 mm are shown in Figures 2.6 to 2.9 respectively.

Figure 2.5 indicates that as the boundary shear displacement δ increases, the net lateral

Table 2.1 Summary of Results on Numerical Direct Shear Box Test and Zone Shear Box Test Simulation

δ (mm)	T_{max} (kN/nail)			M_{max} (kNm/nail)			Ps_{max} (kN/nail)			σ_b (kN/m^2)			l_s (mm)		
	z = 0 mm	z = 100 mm	z = 200 mm	z = 0 mm	z = 100 mm	z = 200 mm	z = 0 mm	z = 100 mm	z = 200 mm	z = 0 mm	z = 100 mm	z = 200 mm	z = 0 mm	z = 100 mm	z = 200 mm
5	0.18 (0.1%)	0.28 (0.1%)	0.26 (0.1%)	0.08 (6.7%)	0.06 (5.0%)	0.06 (5.0%)	1.11 (1.0%)	0.70 (0.6%)	0.59 (0.5%)	350	400	300	300	300	420
10	0.42 (0.2%)	0.60 (0.3%)	0.56 (0.2%)	0.15 (12.5%)	0.11 (9.2 %)	0.10 (8.3%)	1.58 (1.4%)	0.96 (0.8%)	0.81 (0.7%)	400	400	300	400	460	540
25	0.97 (0.4%)	1.12 (0.5%)	0.94 (0.4%)	0.27 (22.5%)	0.24 (20.0%)	0.24 (20.0%)	2.11 (1.9%)	1.55 (1.4%)	1.36 (1.2%)	450	550	450	540	580	650
50	1.50 (0.7%)	1.70 (0.8%)	1.47 (0.7%)	0.44 (36.7%)	0.42 (35.0%)	0.41 (34.2%)	2.81 (2.5%)	2.15 (1.9%)	1.85 (1.4%)	700	850	700	640	740	780

Legend:

T_{max}	Maximum axial force	M_{max}	Maximum bending moment	Ps_{max}	Maximum shear force
l_s	Shear band width	δ	Boundary shear displacement	z	Width of shear zone
σ_b	Lateral soil pressure near the shear plane				

Notes:
(1) Capacity of the soil nail:
Axial capacity, T_p = 226 kN/nail.
Shear capacity, P_s = 113 kN/nail.
Moment capacity, M_p = 1.2 kNm/nail.
(2) The figures in the brackets are the numerical results compared with the corresponding capacities.

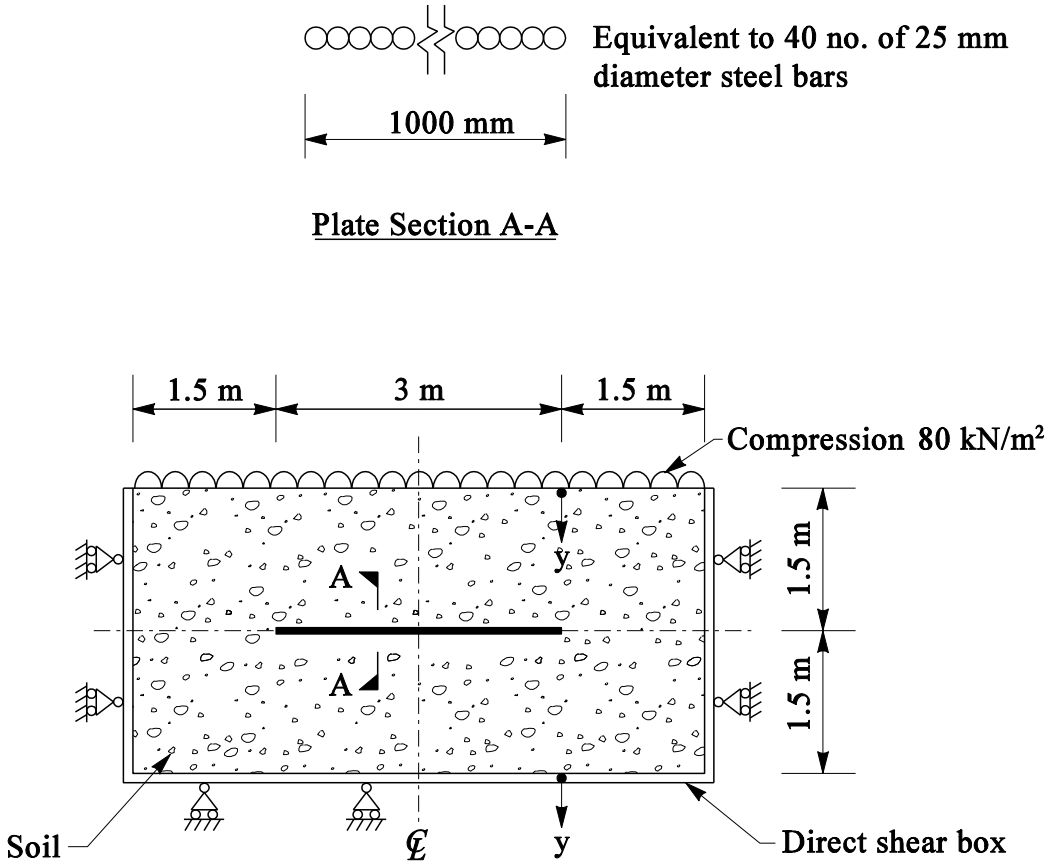

Steel plate size: Equivalent to 40 no. x 25 mm diameter steel bar x 3 m (length)

Steel plate parameters

σ_y = 460 N/mm²
E_{steel} = 205 kN/mm²

Soil sample size: 6 m (length) x 1 m (width) x 3 m (depth)

Soil parameters:

c' = 0 kN/m²
ϕ' = 40°
γ = 16 kN/m³
E_{soil} = 60 MN/m²
ν = 0.4

Prescribed downward boundary shear displacement δ along y-axis = 0, 5, 25, 50 mm at the RHS of the shear box

Figure 2.4 Details of Numerical Direct Shear Box Test Simulation

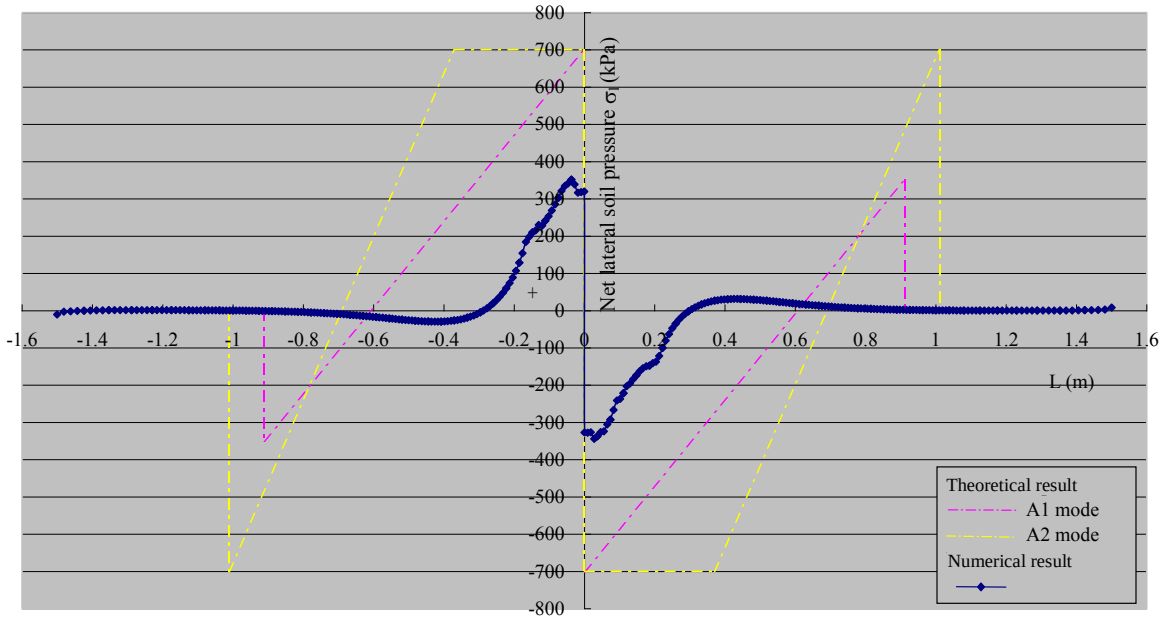

(a) Boundary Shear Displacement, δ = 5 mm

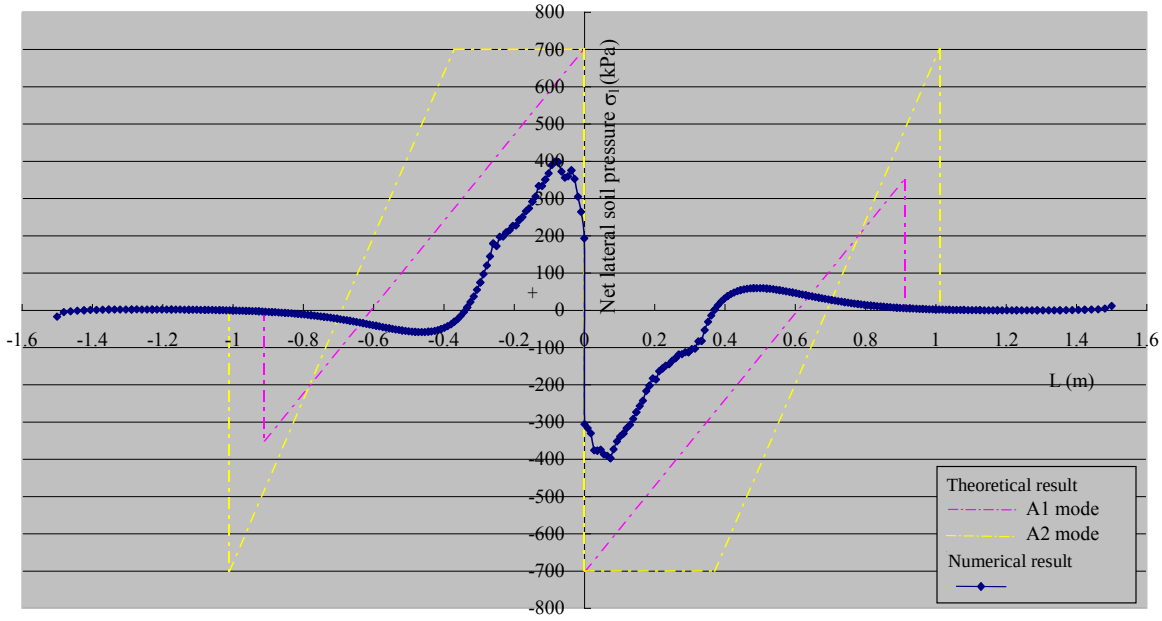

(b) Boundary Shear Displacement, δ = 10 mm

Figure 2.5 Net Lateral Soil Pressure Distribution along the Soil Nail in Numerical Direct Shear Box Test Simulation (Sheet 1 of 2)

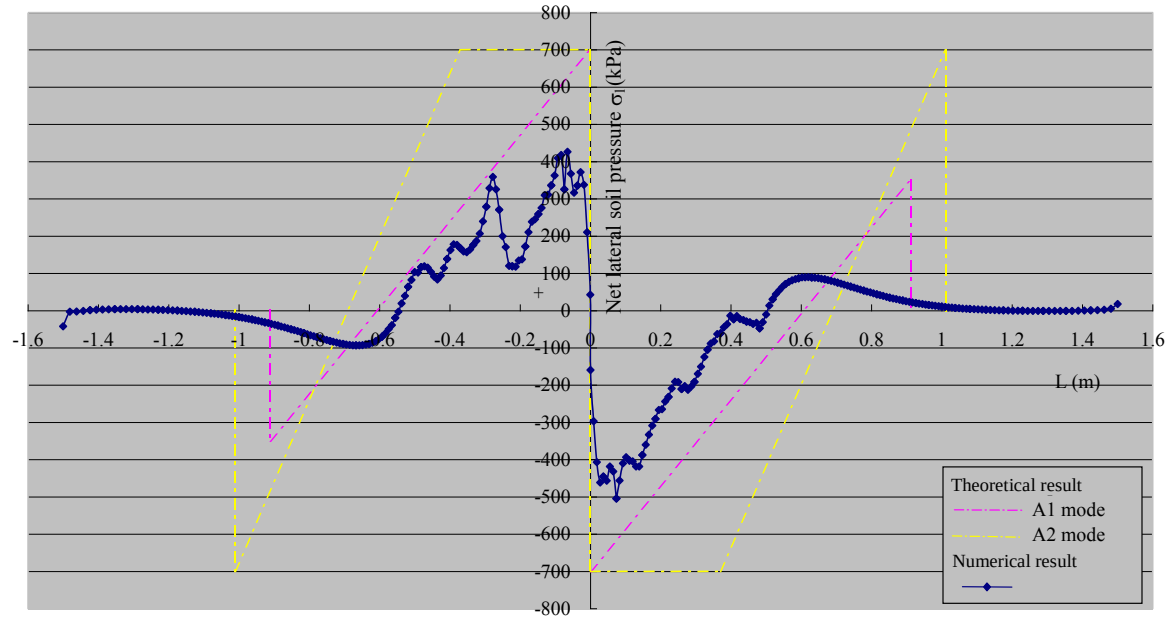

(c) Boundary Shear Displacement, δ = 25 mm

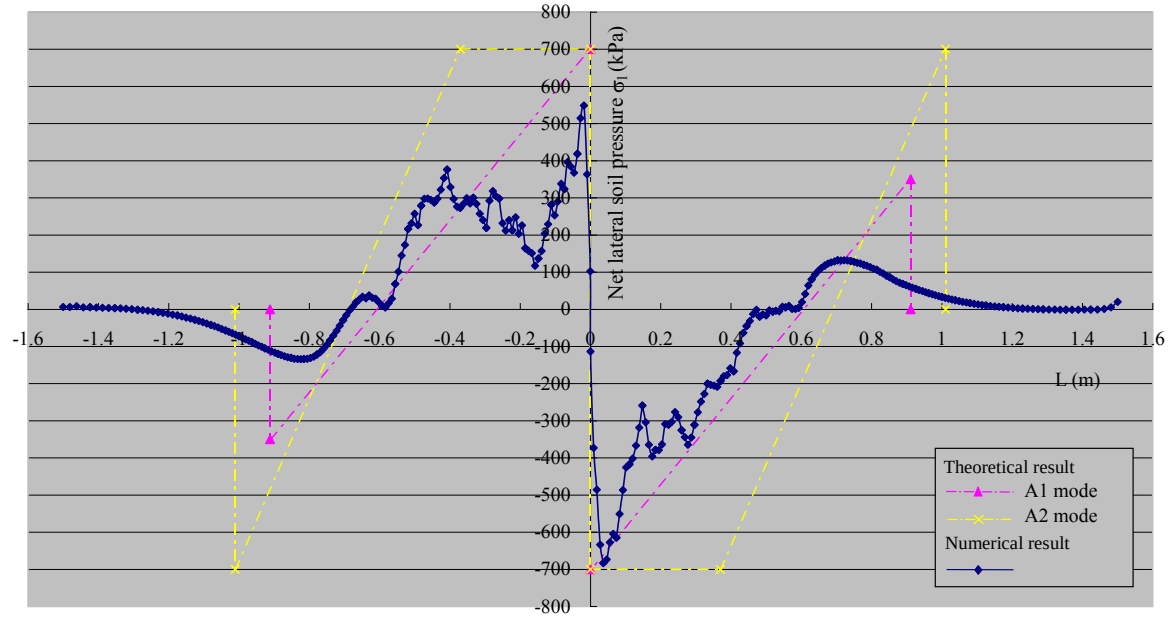

(d) Boundary Shear Displacement, δ = 50 mm

Figure 2.5 Net Lateral Soil Pressure Distribution along the Soil Nail in Numerical Direct Shear Box Test Simulation (Sheet 2 of 2)

soil pressure increases. Although the distributions of the net lateral soil pressure generally resemble those of the theoretical values, there are high fluctuations of the distribution when the boundary shear displacement increases, in particular when δ was increased to 25 mm or 50 mm.

Table 2.1 shows that as the boundary shear displacement increases, the maximum values of shear force, bending moment and axial forces increase. However, the maximum axial force and shear force that were mobilised in the nail reinforcement when δ = 50 mm were only 0.7% and 2.5% of their respective capacity, compared with 36.7% of bending moment. This suggests that the bending capacity would be reached prior to the reaching of shear or tensile capacity as the shearing process continues. In other words, bending failure mechanism is the critical failure mode if a steel soil nail is subjected to plane shearing. This finding is consistent with the observations in the mode of failure of the nail reinforcement in landslides. In the previous cases of temporary soil-nailed slope failures, some steel nail bars were bent; no shear rupture of the reinforcement was seen.

One should caution that in order to examine the element behaviour of the nail reinforcement under shearing, the reinforcement was purposely placed normal to the shear plane in the numerical simulation. As a result, the reinforcement was orientated away from the direction of the principle tensile strain in the soil. This represents the worst scenario in respect of maximum bending moment and shear force, and only small axial force would be mobilised. Where soil nails are orientated close to the direction of principle tensile strain in the soil, previous study by Jewell & Pedley (1992) shows that mobilisation of shear stresses and bending moments of soil nails are small under service load conditions. One may also notice from Figures 2.6 to 2.9 that the zone of bending increases when the boundary shear displacement increases, and it is about half metre each from the shearing plane.

As the axial force, bending moment and shear force of the nail reinforcement were obtained from 2-dimensional analysis, the values are likely on the high side when compared with those from 3-dimensional analysis. It is because in 2-dimensional analysis, the nail reinforcement is forced to resist the movement of soil in the shear box during shearing, whereas in 3-dimensional analysis, soil is allowed to "flow" between reinforcement bars.

2.2.4 Modelling of Shear Zone

2.2.4.1 Numerical Model - Zone Shear Box Test

To model the effect of shear zone on the nail-soil interaction, the numerical direct shear box model described in Section 2.2.3.1 was modified to a zone shear box as shown in Figure 2.10. Shear zones of width, *z*, 100 mm and 200 mm, were investigated in the study. In the loading process, a linearly varying downward displacement was applied across the shear zone width spanning symmetrically across the two halves of the box, whilst an imposed uniform boundary shear displacement, δ, of 5 mm, 10 mm, 25 mm and 50 mm was applied in sequence in the downward direction y beyond the shear zone along the top and bottom of the right half of the box.

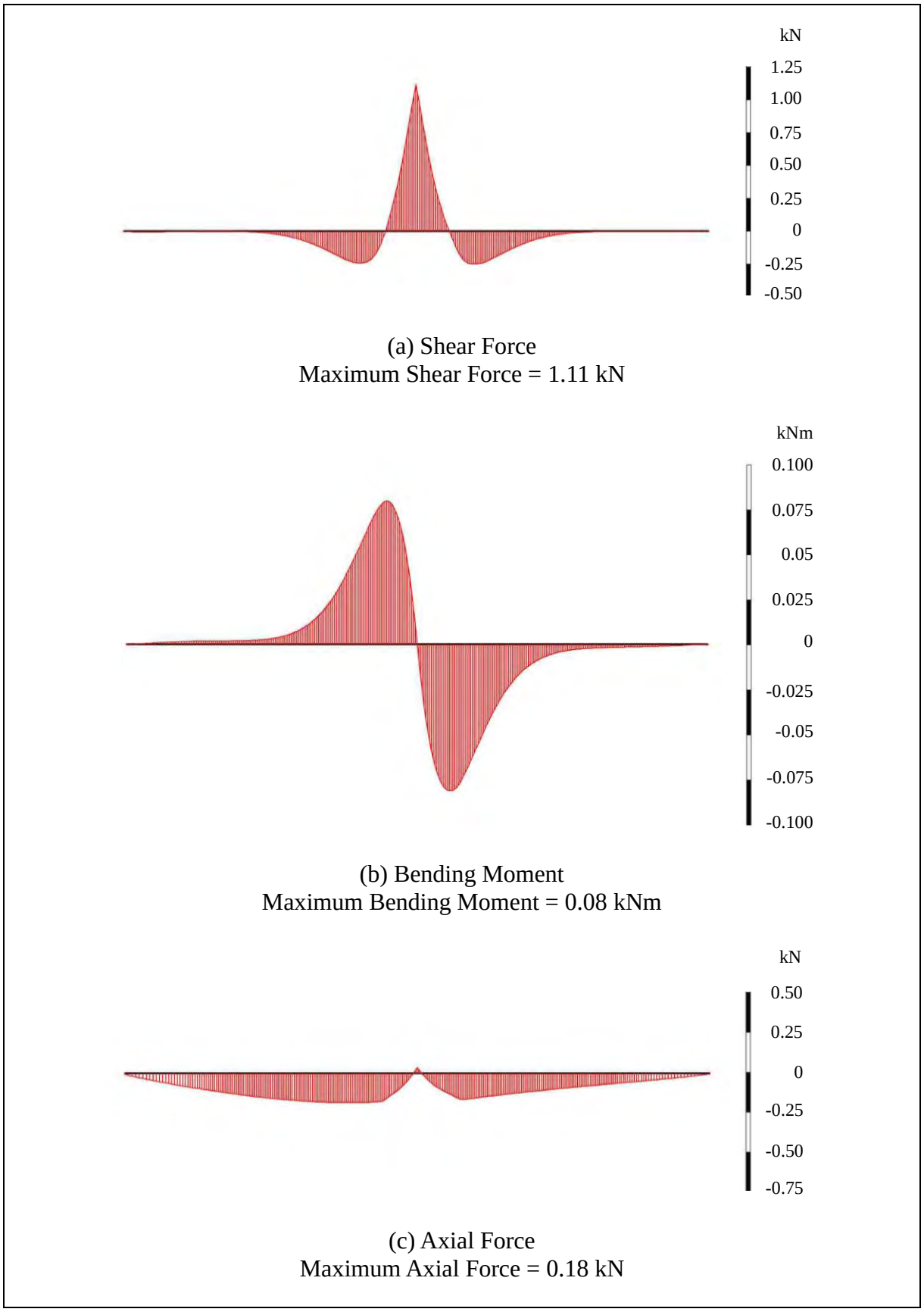

Figure 2.6 Distributions of Shear Force, Bending Moment and Axial Force along the Soil Nail in the Numerical Direct Shear Box Test Simulation When δ = 5 mm

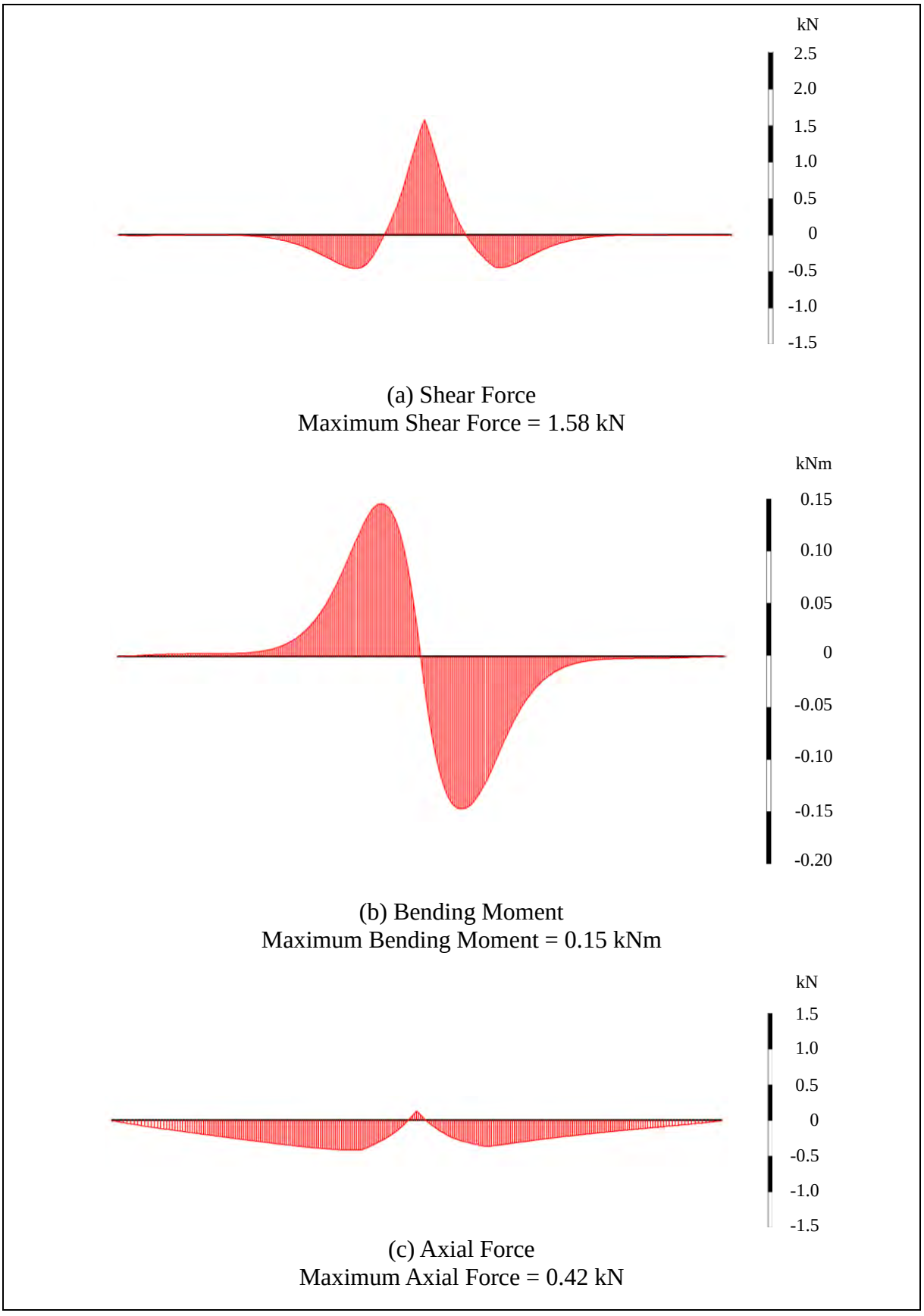

Figure 2.7 Distributions of Shear Force, Bending Moment and Axial Force along the Soil Nail in the Numerical Direct Shear Box Test Simulation When δ = 10 mm

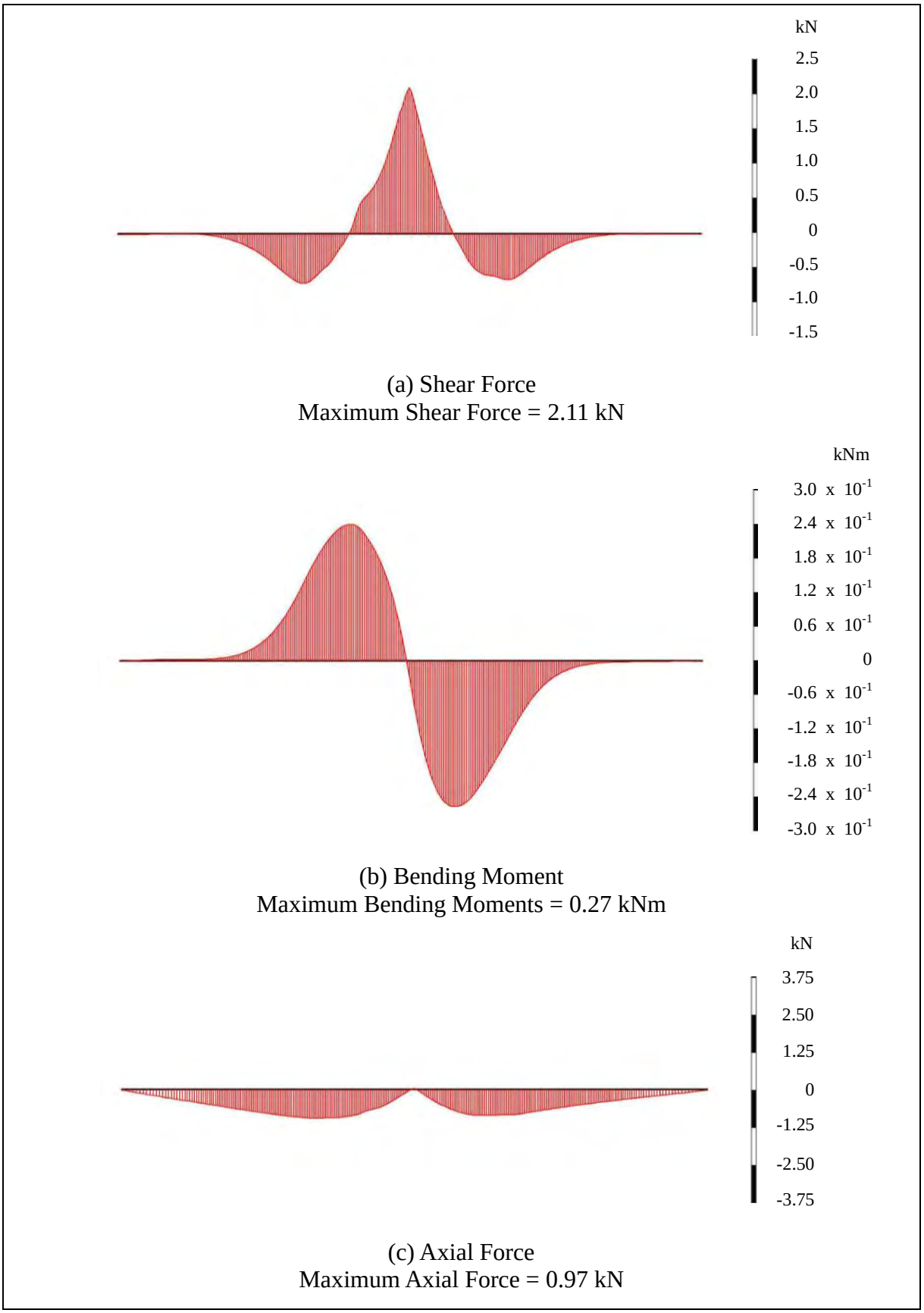

Figure 2.8 Distributions of Shear Force, Bending Moment and Axial Force along the Soil Nail in the Numerical Direct Shear Box Test Simulation When δ = 25 mm

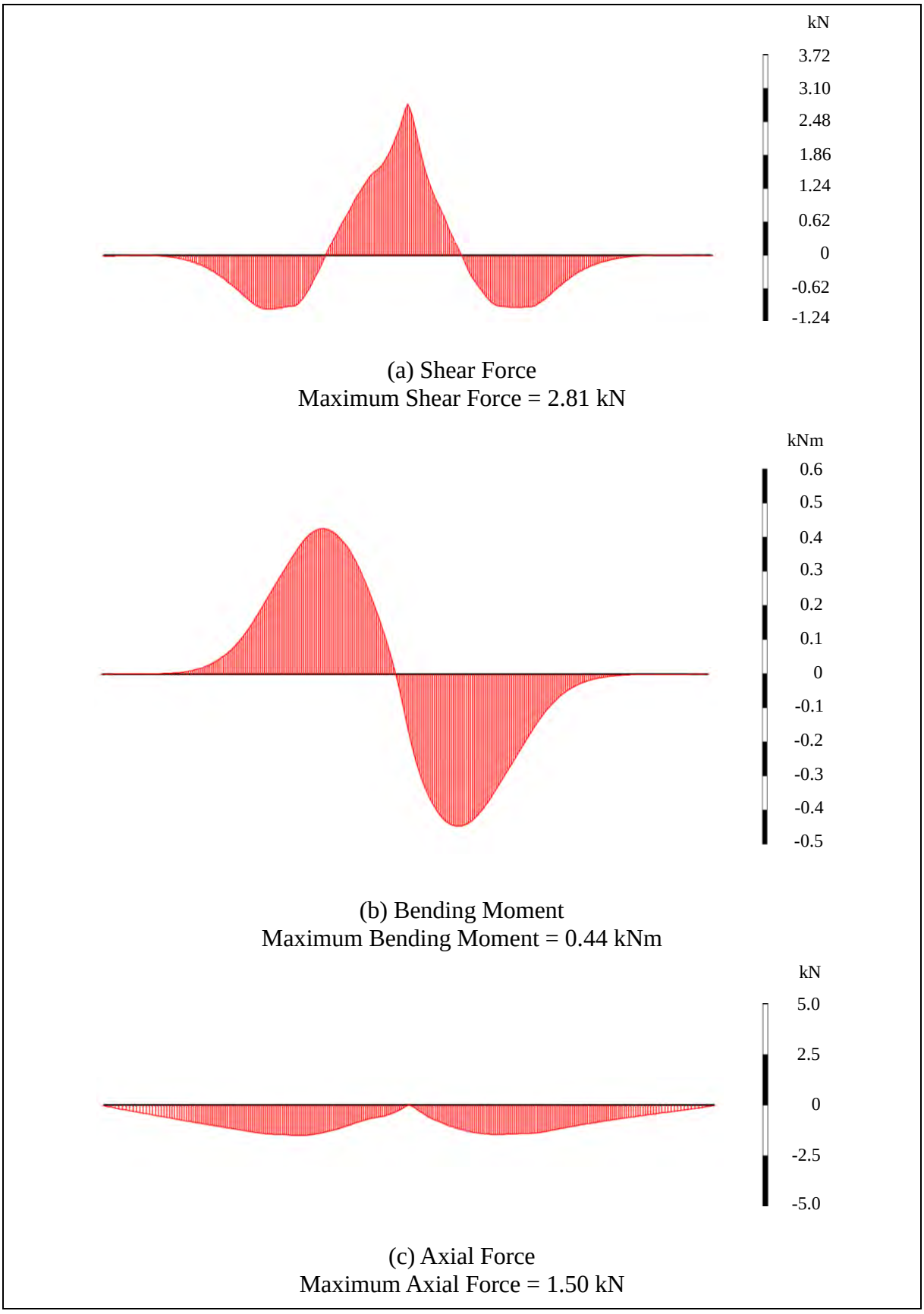

Figure 2.9 Distributions of Shear Force, Bending Moment and Axial Force along the Soil Nail in the Numerical Direct Shear Box Test Simulation When δ = 50 mm

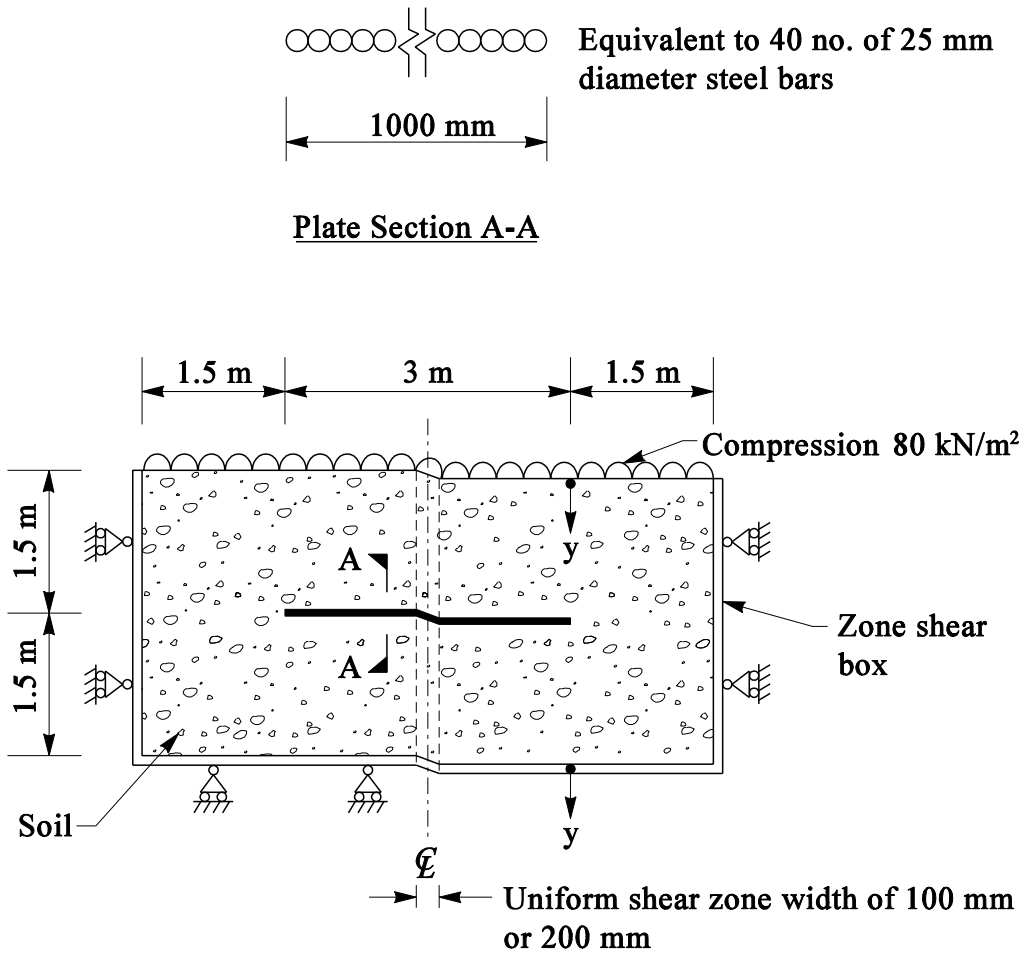

Steel plate size: Equivalent to 40 no. x 25 mm diameter steel bar x 3 m (length)

Steel plate parameters

σ_y = 460 N/mm²
E_{steel} = 205 kN/mm²

Soil sample size: 6 m (length) x 1 m (width) x 3 m (depth)

Soil parameters:

c' = 0 kN/m²
ϕ' = 40°
γ = 16 kN/m³
E_{soil} = 60 MN/m²
ν = 0.4

Prescribed downward boundary shear displacement δ along y-axis = 0, 5, 25, 50 mm at the RHS of the shear box

Figure 2.10 Details of Numerical Zone Shear Box Test Simulation

2.2.4.2 Results and Discussions

For each width of shear zone and for each imposed boundary shear displacement δ, the net lateral soil pressures σ_l obtained from the numerical simulations are shown in Figures 2.11 and 2.12. The theoretical net lateral soil pressure distributions for failure modes A1 and A2 are also plotted in the figures for comparison.

The maximum shear force Ps_{max}, maximum bending moment M_{max} and maximum axial force T_{max} of nail reinforcement corresponding to boundary shear displacement δ of 5 mm, 10 mm, 25 mm and 50 mm for each shear zone width are shown in Table 2.1. The distributions of shear force, bending moment and axial force along the soil nail corresponding to boundary shear displacement δ of 5 mm, 10 mm, 25 mm and 50 mm for each shear zone width are shown in Figures 2.13 to 2.20 respectively.

Figures 2.11 and 2.12 indicate that as the boundary shear displacement δ increases, the net lateral soil pressure increases. Similar to those of numerical direct shear box test simulations, the distributions of the net lateral soil pressure at small displacements generally resemble those of the theoretical values, and there are high fluctuations of the distribution when the boundary shear displacement increases, in particular when δ was increased to 25 mm or 50 mm. In addition, for a given boundary shear displacement, the net lateral soil pressure increases as the width of shear zone decreases. Similar observations are made for the maximum values of shear force, bending moment and axial forces as summarised in Table 2.1.

Table 2.1 shows that irrespective of the width of shear zone, as the boundary shear displacement increases, the maximum values of shear force, bending moment and axial forces increase. However, the maximum axial force and shear force that were mobilised in the nail reinforcement when δ = 50 mm were only 0.7% and 2.5% of their respective capacity, compared with 36.7% of bending moment. This suggests that the bending capacity would be reached prior to the reaching of shear or tensile capacity as the shearing process continues. In other words, bending failure mechanism is the critical failure mode if a steel soil nail is subjected to plane shearing.

2.2.5 Modelling of Ground with Contrast in Stiffness

In order to understand the nail-soil interaction in the case of a soil nail passing through two soil materials with different soil stiffness, further numerical simulations using the direct shear box model as described in Section 2.2.3.1 were conducted. Two cases were examined. In both cases, the original soil stiffness of 60 MN/m^2 was kept unchanged in the right half of the box. In the left half, the stiffness of the soil was increased to 120 MN/m^2 and 600 MN/m^2 respectively. The details of the model shear box, and the soil and steel parameters are given in Figure 2.21.

2.2.5.1 Results and Discussions

The results are summarised in Table 2.2. In general, the maximum shear force, bending moment and axial force, and the net lateral soil pressure near the shear plane increase as the contrast in soil stiffness increases as well as the boundary shear displacement increases.

Table 2.2 Summary of Results on Numerical Direct Shear Box Test Simulations with Soils of Contrast in Stiffness

δ (mm)	T_{max} (kN/nail)			M_{max} (kNm/nail)			Ps_{max} (kN/nail)			σ_b (kN/m^2)		
	E_{soil} = 60 MN/m^2 (Note 1)	E_{soil} = 120 MN/m^2	E_{soil} = 600 MN/m^2	E_{soil} = 60 MN/m^2 (Note 1)	E_{soil} = 120 MN/m^2	E_{soil} = 600 MN/m^2	E_{soil} = 60 MN/m^2 (Note 1)	E_{soil} = 120 MN/m^2	E_{soil} = 600 MN/m^2	E_{soil} = 60 MN/m^2 (Note 1)	E_{soil} = 120 MN/m^2	E_{soil} = 600 MN/m^2
5	0.18 (0.1%)	0.27 (0.1%)	0.56 (0.2%)	0.08 (6.7%)	0.11 (9.2%)	0.13 (10.8%)	1.11 (1.0%)	1.27 (1.1%)	1.31 (1.2%)	350	362	468
10	0.42 (0.2%)	0.58 (0.3%)	0.81 (0.4%)	0.15 (12.5%)	0.17 (14.2%)	0.18 (15.0%)	1.58 (1.4%)	1.66 (1.5%)	1.64 (1.4%)	400	415	491
25	0.97 (0.4%)	1.04 (0.5%)	1.46 (0.6%)	0.27 (22.5%)	0.28 (23.3%)	0.30 (25.0%)	2.11 (1.9%)	2.16 (1.9%)	2.25 (2.0%)	450	536	599
50	1.50 (0.7%)	1.73 (0.8%)	NC	0.44 (36.7%)	0.48 (40.0%)	NC	2.81 (2.5%)	2.94 (2.6%)	NC	700	782	NC

Legend:

T_{max}	Maximum axial force	δ	Boundary shear displacement	M_{max}	Maximum bending moment
E_{soil}	Soil stiffness in the left-half of the shear box	Ps_{max}	Maximum shear force	NC	Non-convergent
σ_b	Lateral soil pressure near the shear plane				

Notes:

(1) Results of numerical direct shear box test simulations without contrast in soil stiffness.

(2) The capacity of the soil nail:
Axial capacity, T_p = 226 kN/nail.
Shear capacity, P_s = 113 kN/nail.
Moment capacity, M_p = 1.2 kNm/nail.

(3) The figures in the brackets are the numerical results compared with the corresponding capacities.

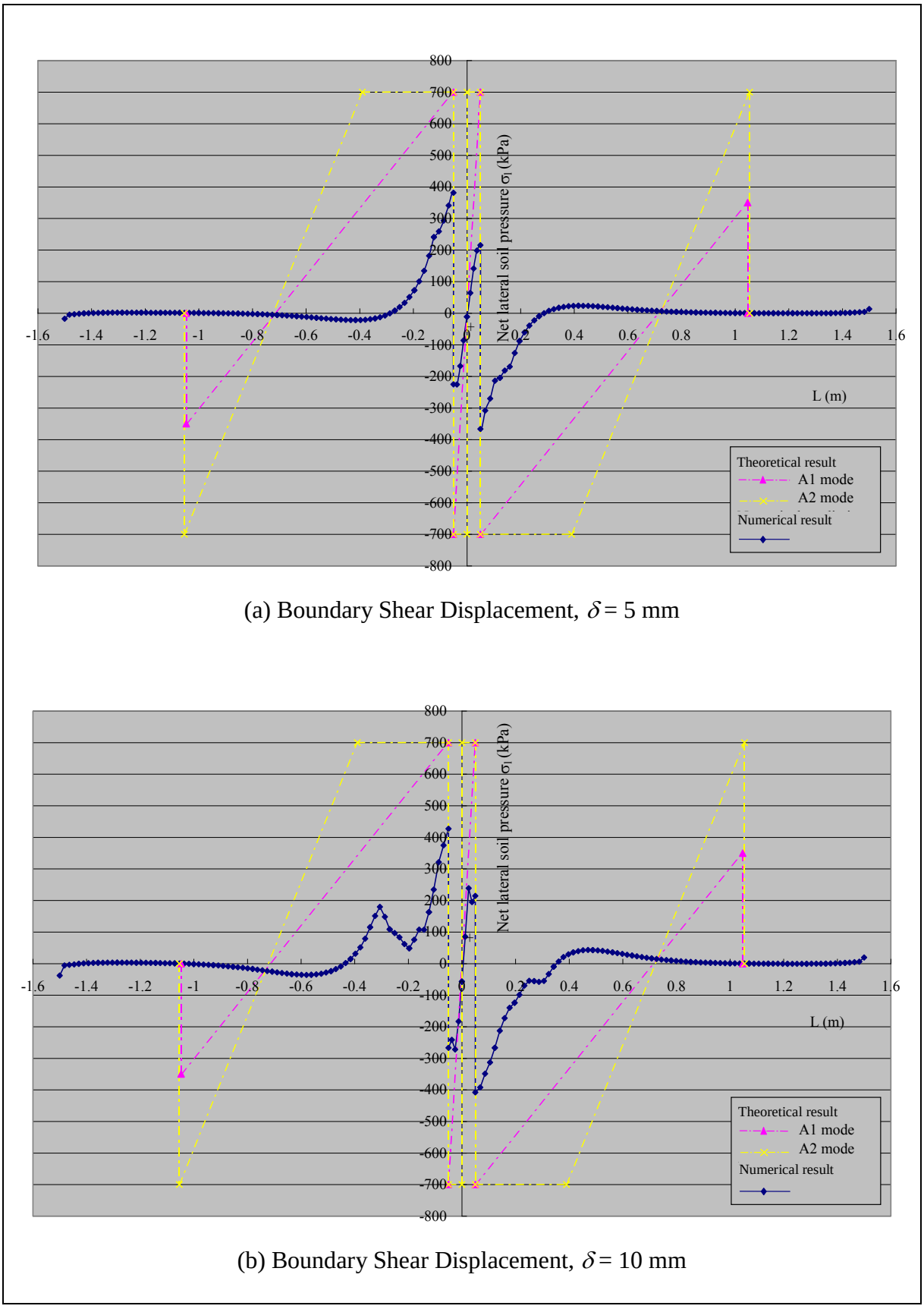

(a) Boundary Shear Displacement, δ = 5 mm

(b) Boundary Shear Displacement, δ = 10 mm

Figure 2.11 Net Lateral Soil Pressure Distribution along the Soil Nail in 100 mm Numerical Zone Shear Box Test Simulation (Sheet 1 of 2)

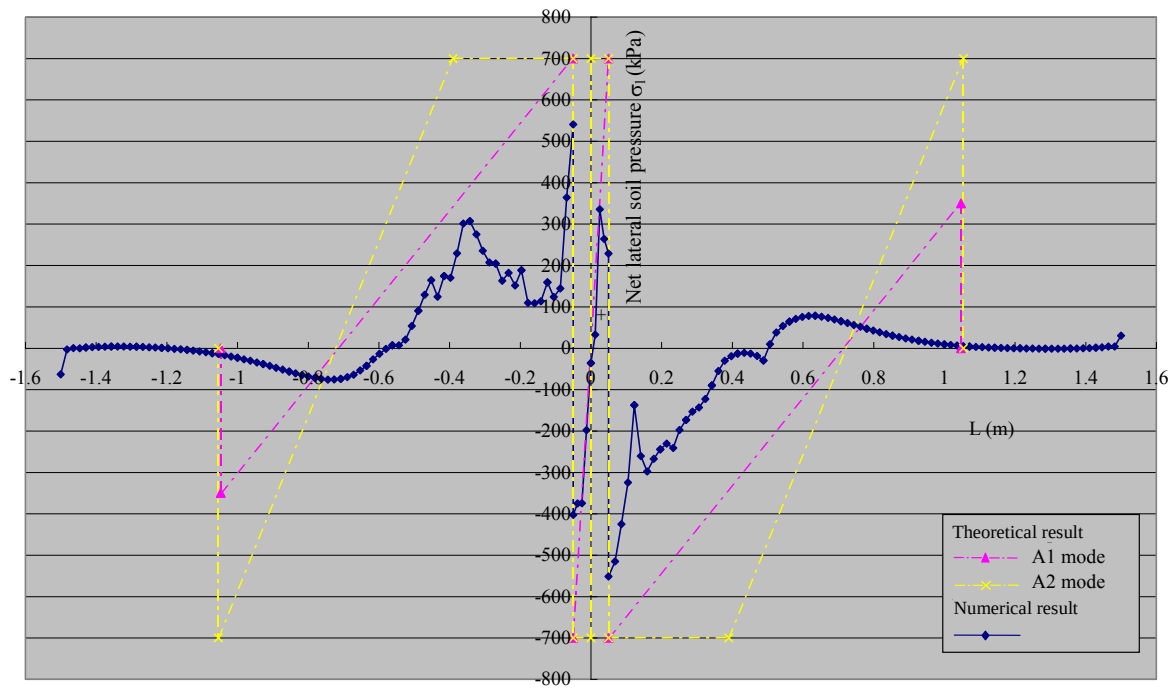

(c) Boundary Shear Displacement, δ = 25 mm

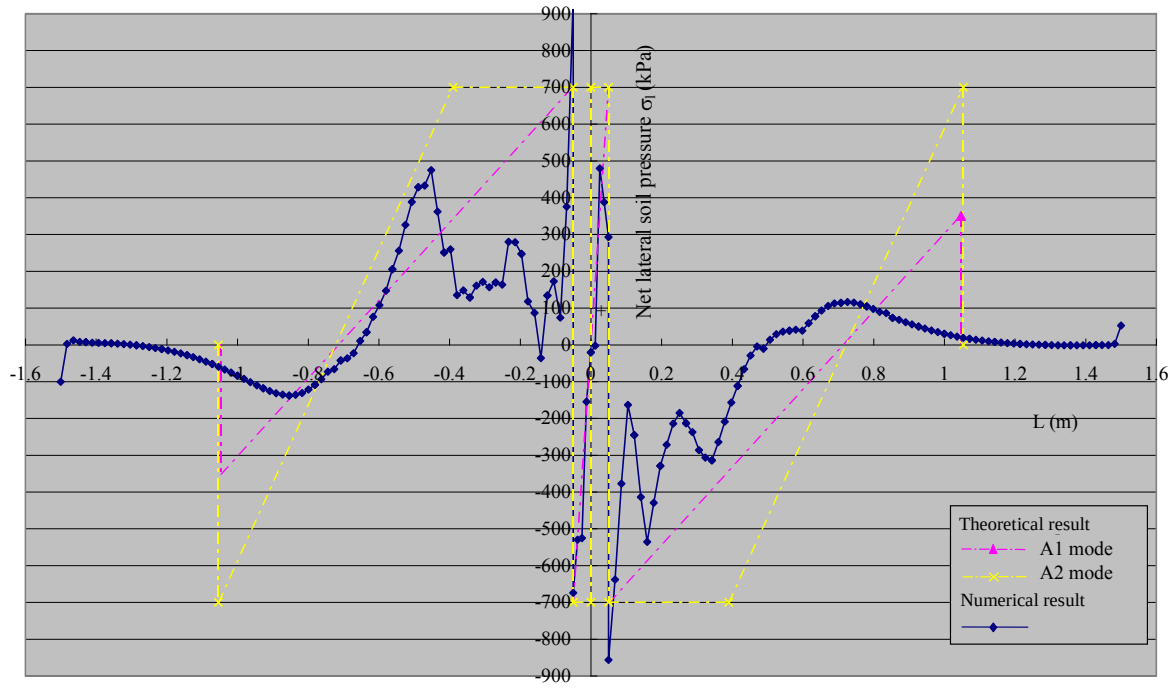

(d) Boundary Shear Displacement, δ = 50 mm

Figure 2.11 Net Lateral Soil Pressure Distribution along the Soil Nail in 100 mm Numerical Zone Shear Box Test Simulation (Sheet 2 of 2)

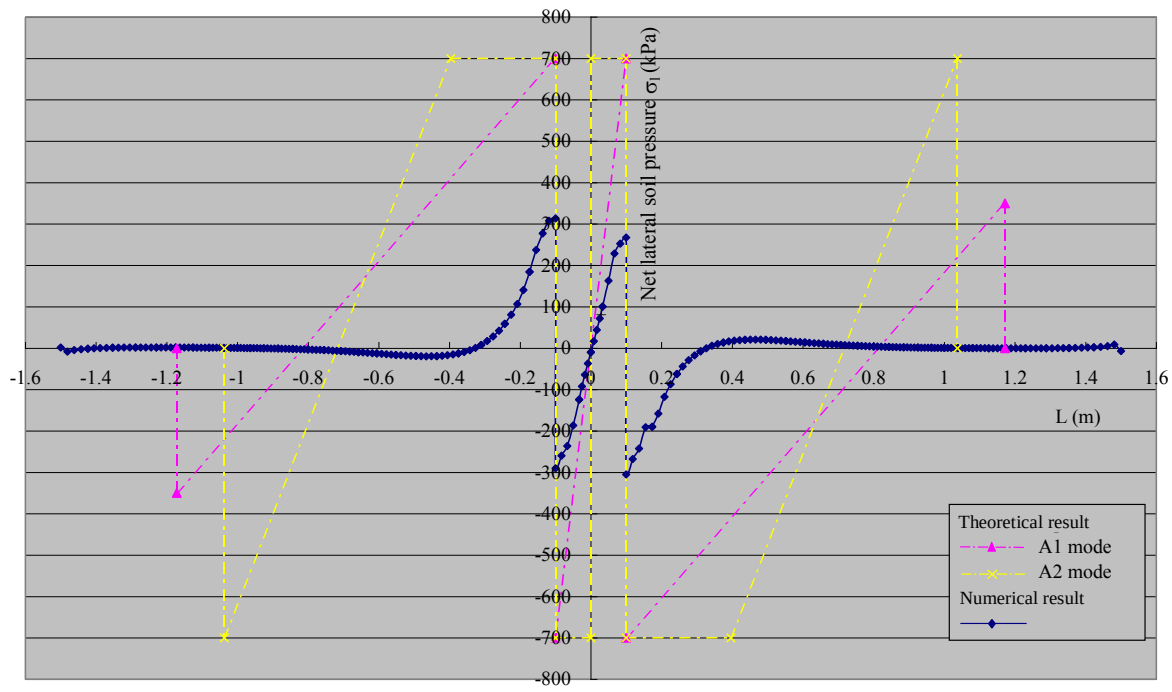

(a) Boundary Shear Displacement, δ = 5 mm

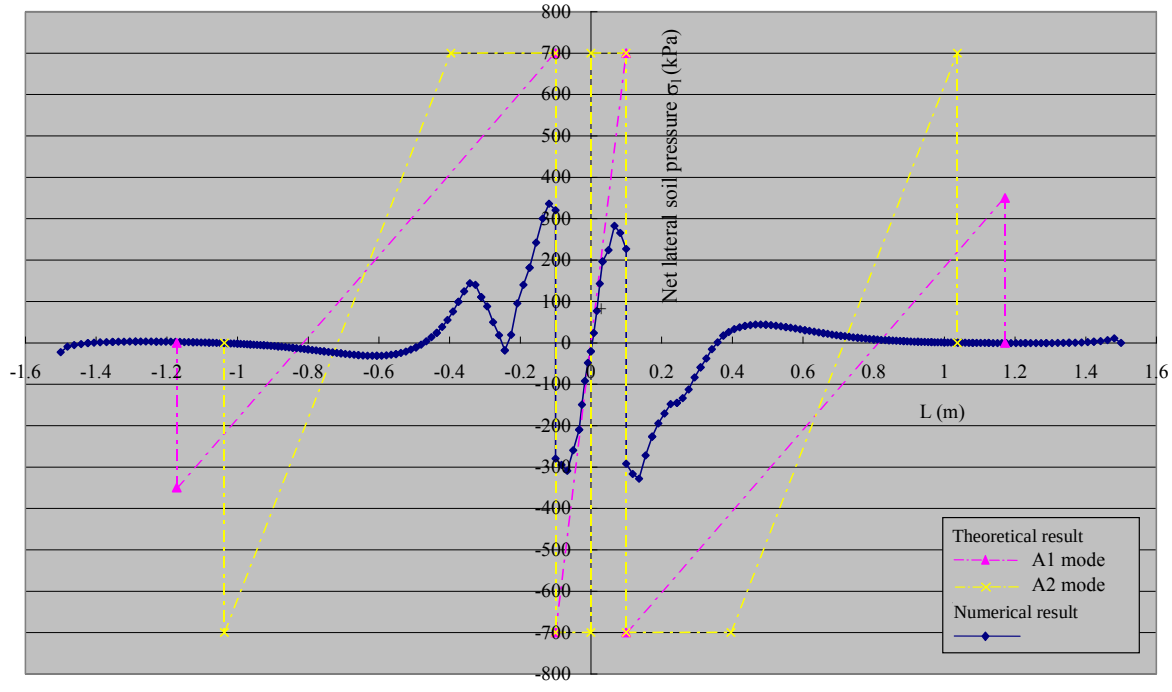

(b) Boundary Shear Displacement, δ = 10 mm

Figure 2.12 Net Lateral Soil Pressure Distribution along the Soil Nail in 200 mm Numerical Zone Shear Box Test Simulation (Sheet 1 of 2)

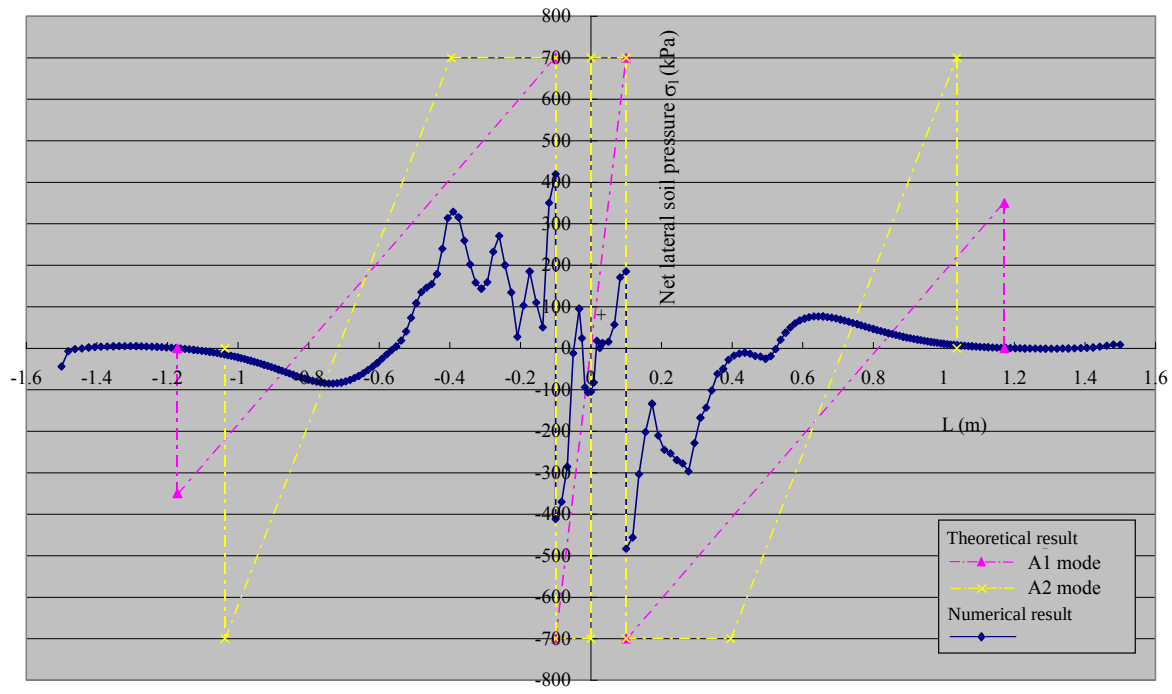

(c) Boundary Shear Displacement, δ = 25 mm

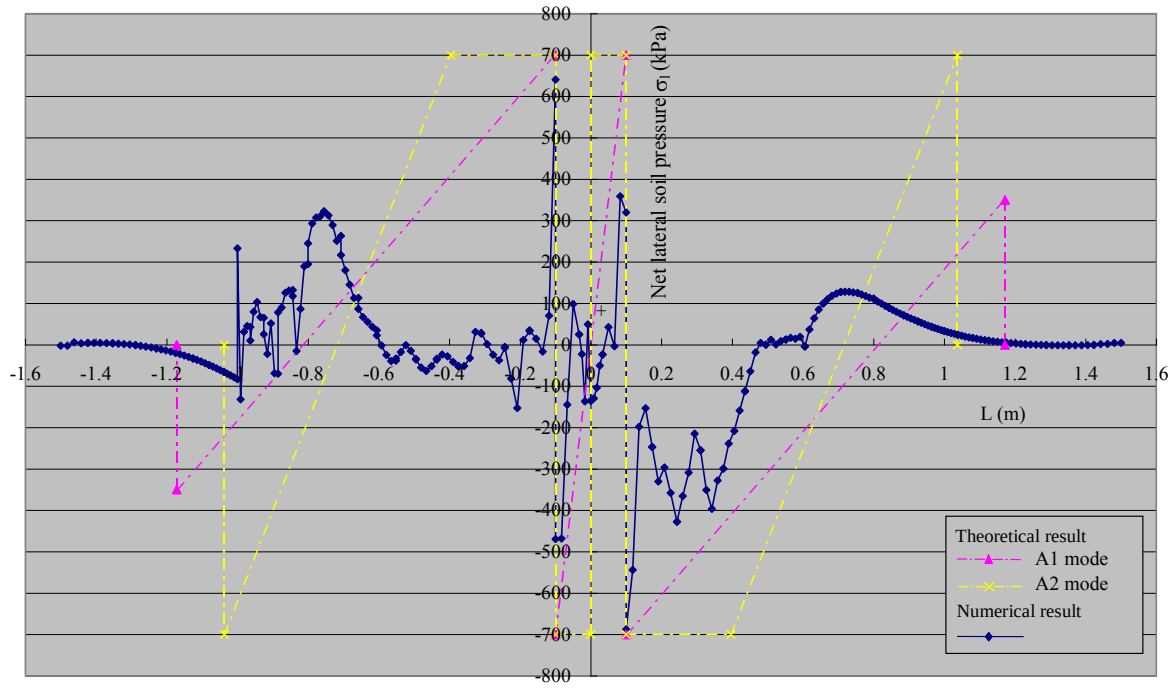

(d) Boundary Shear Displacement, δ = 50 mm

Figure 2.12 Net Lateral Soil Pressure Distribution along the Soil Nail in 200 mm Numerical Zone Shear Box Test Simulation (Sheet 2 of 2)

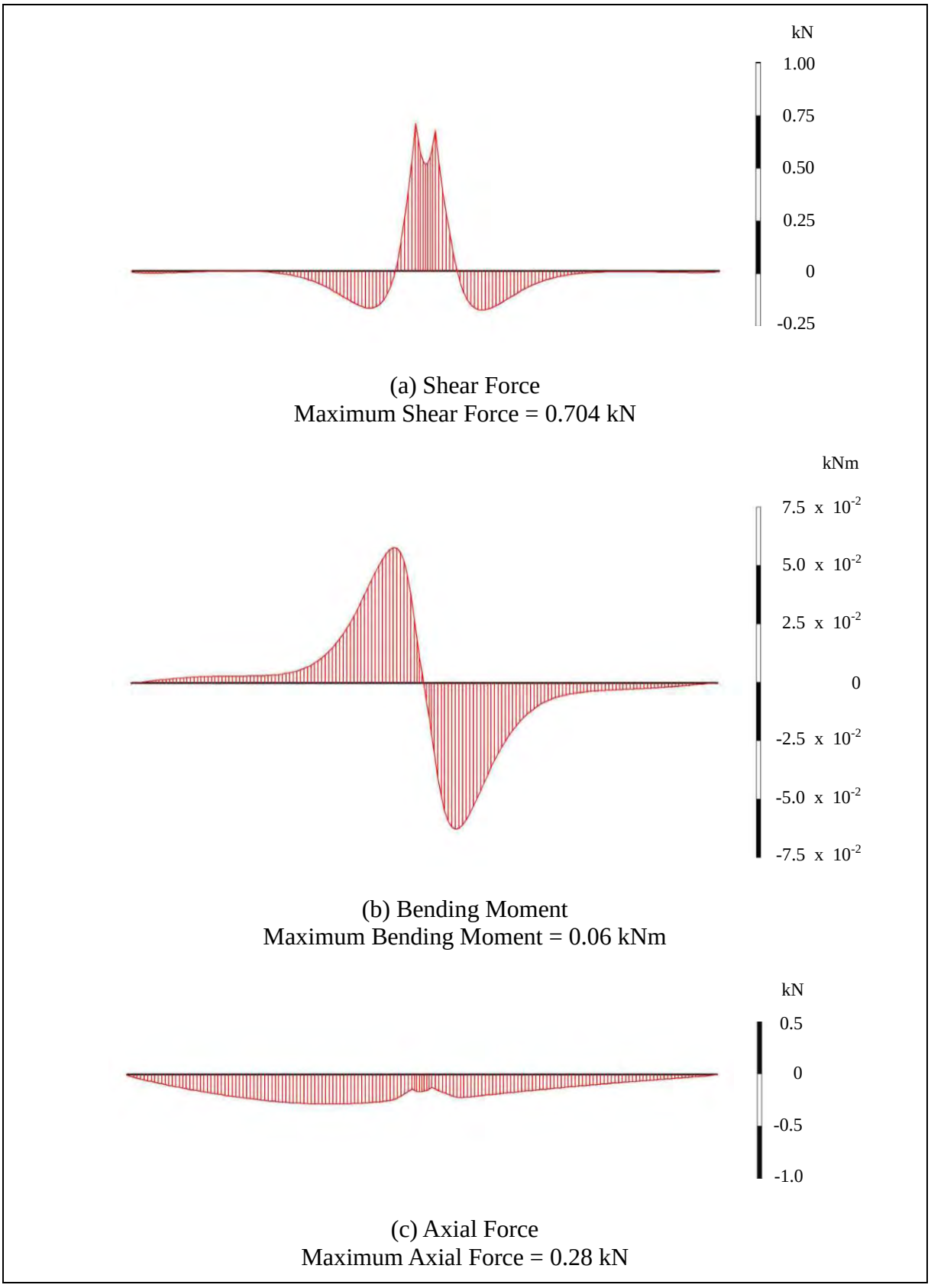

Figure 2.13 Distributions of Shear Force, Bending Moment and Axial Force along the Soil Nail in the 100 mm Zone Numerical Shear Box Test Simulation When δ = 5 mm

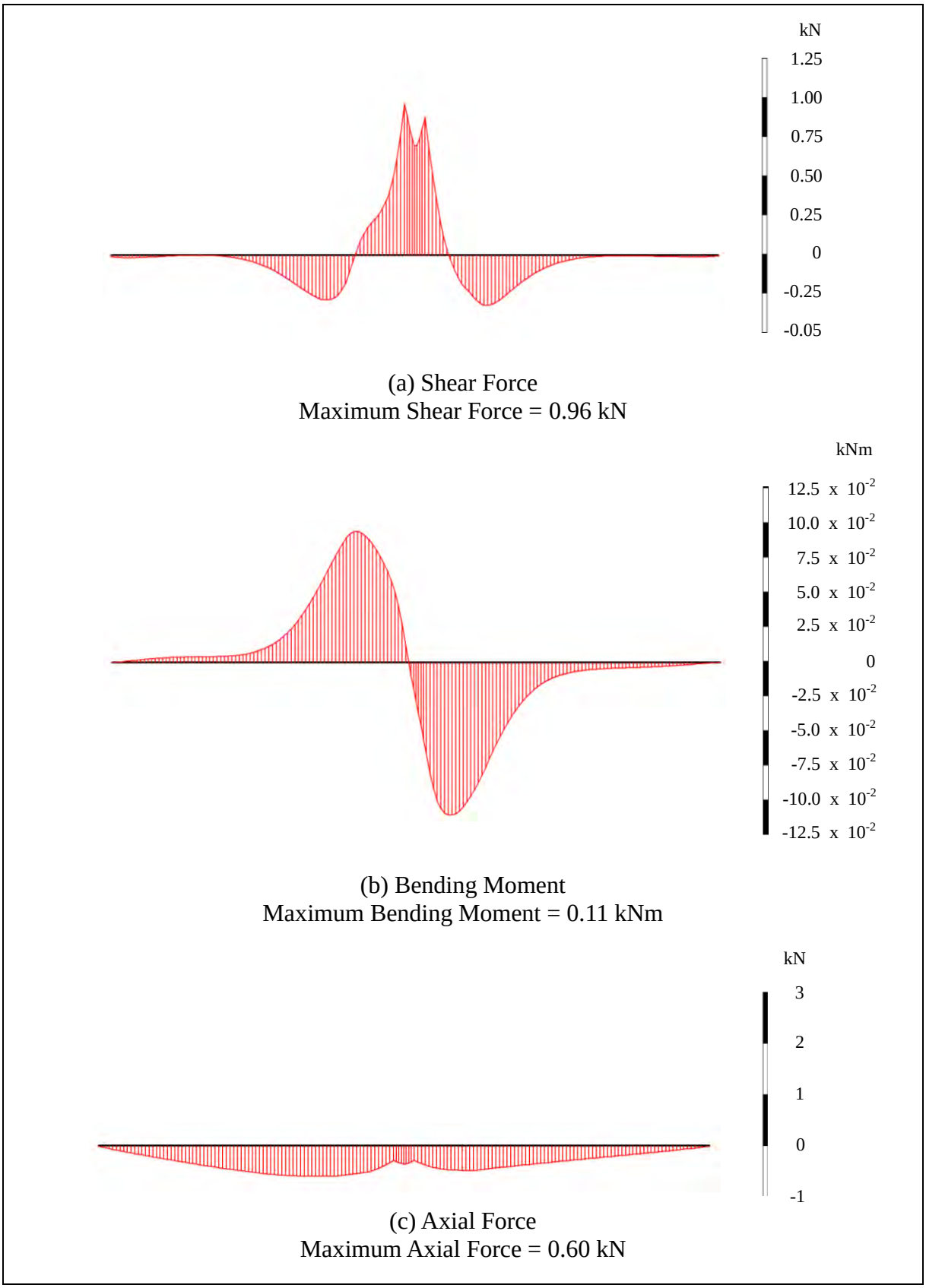

Figure 2.14 Distributions of Shear Force, Bending Moment and Axial Force along the Soil Nail in the 100 mm Zone Numerical Shear Box Test Simulation When δ = 10 mm

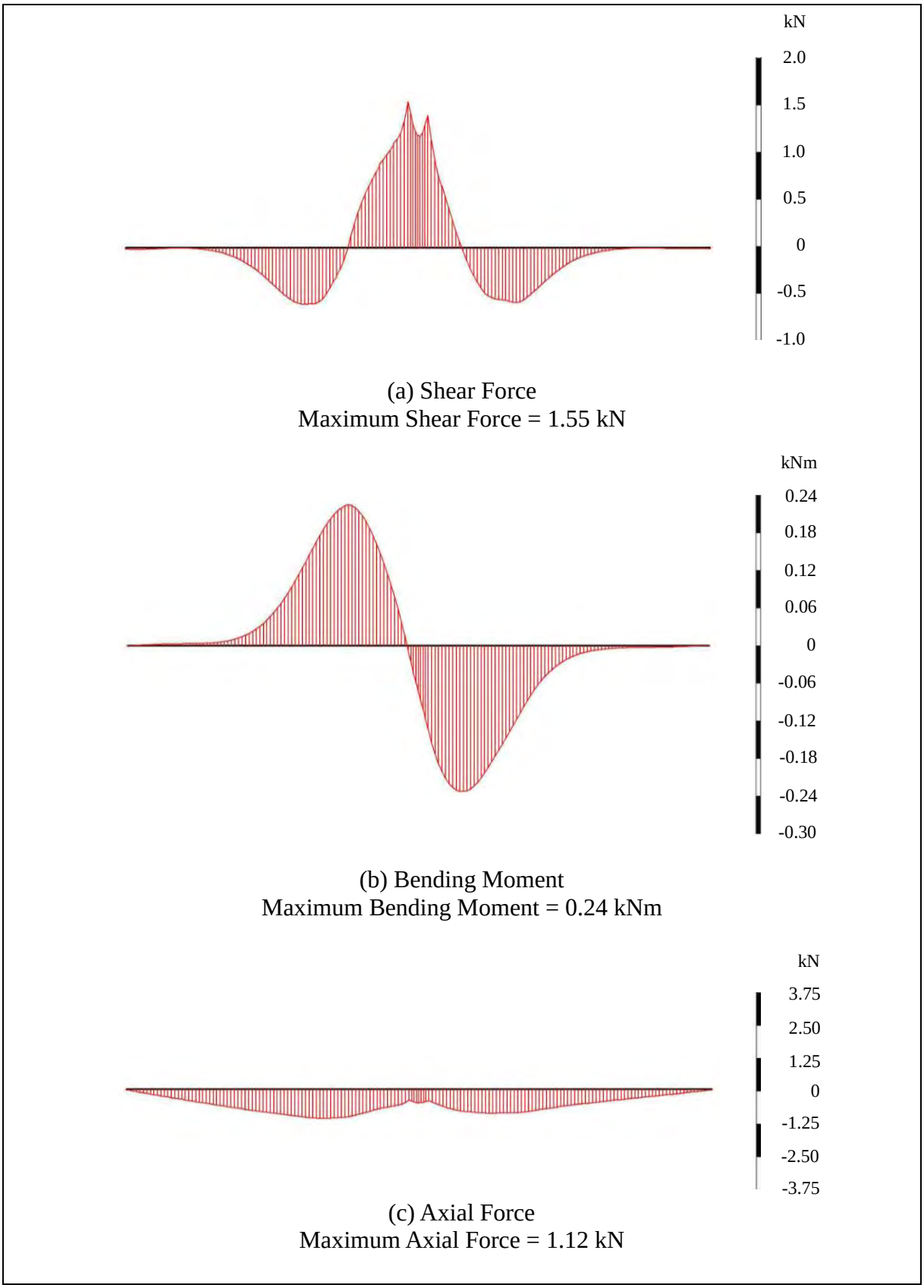

Figure 2.15 Distributions of Shear Force, Bending Moment and Axial Force along the Soil Nail in the 100 mm Zone Numerical Shear Box Test Simulation When δ = 25 mm

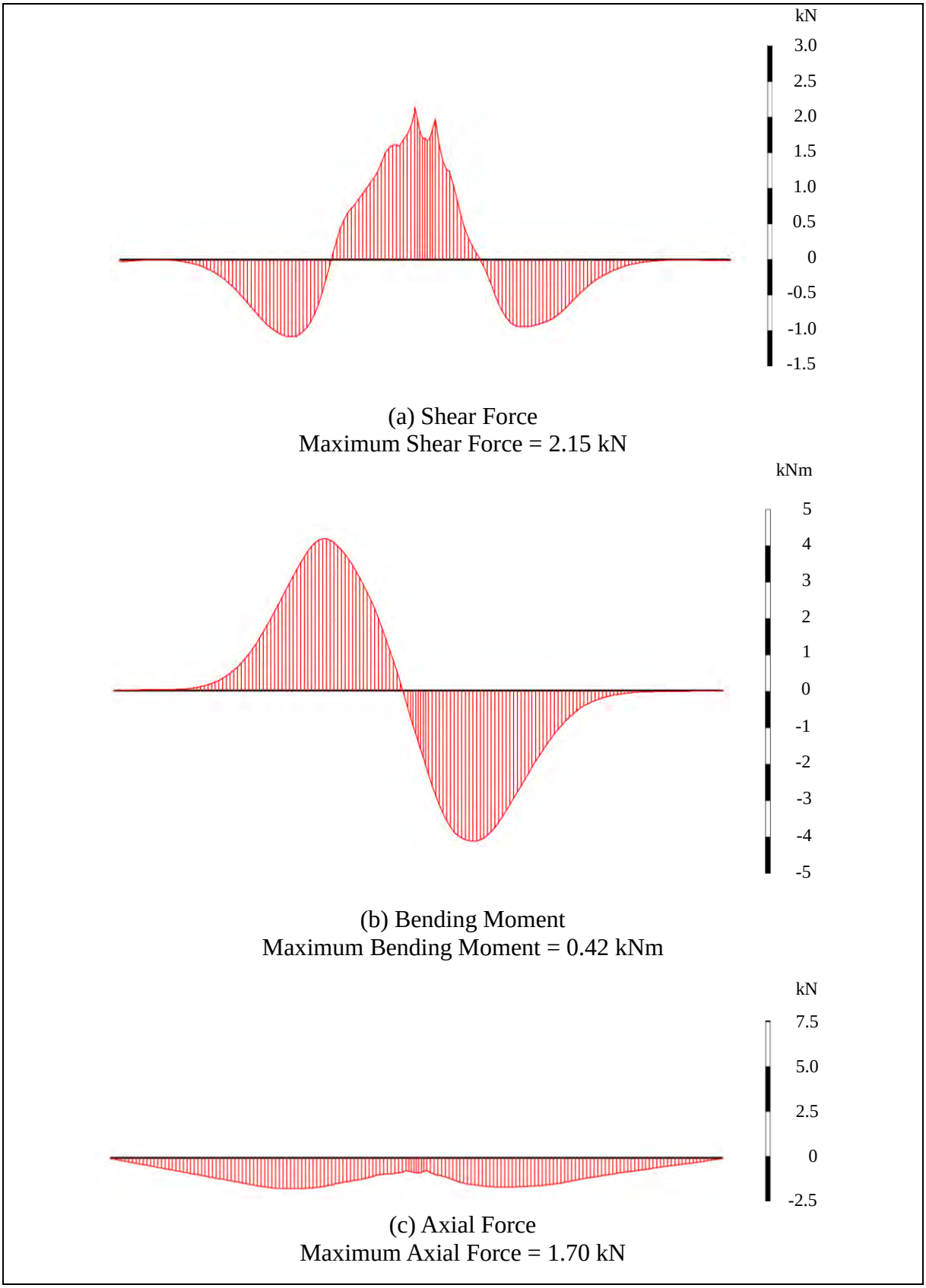

Figure 2.16 Distributions of Shear Force, Bending Moment and Axial Force along the Soil Nail in the 100 mm Zone Numerical Shear Box Test Simulation When δ = 50 mm

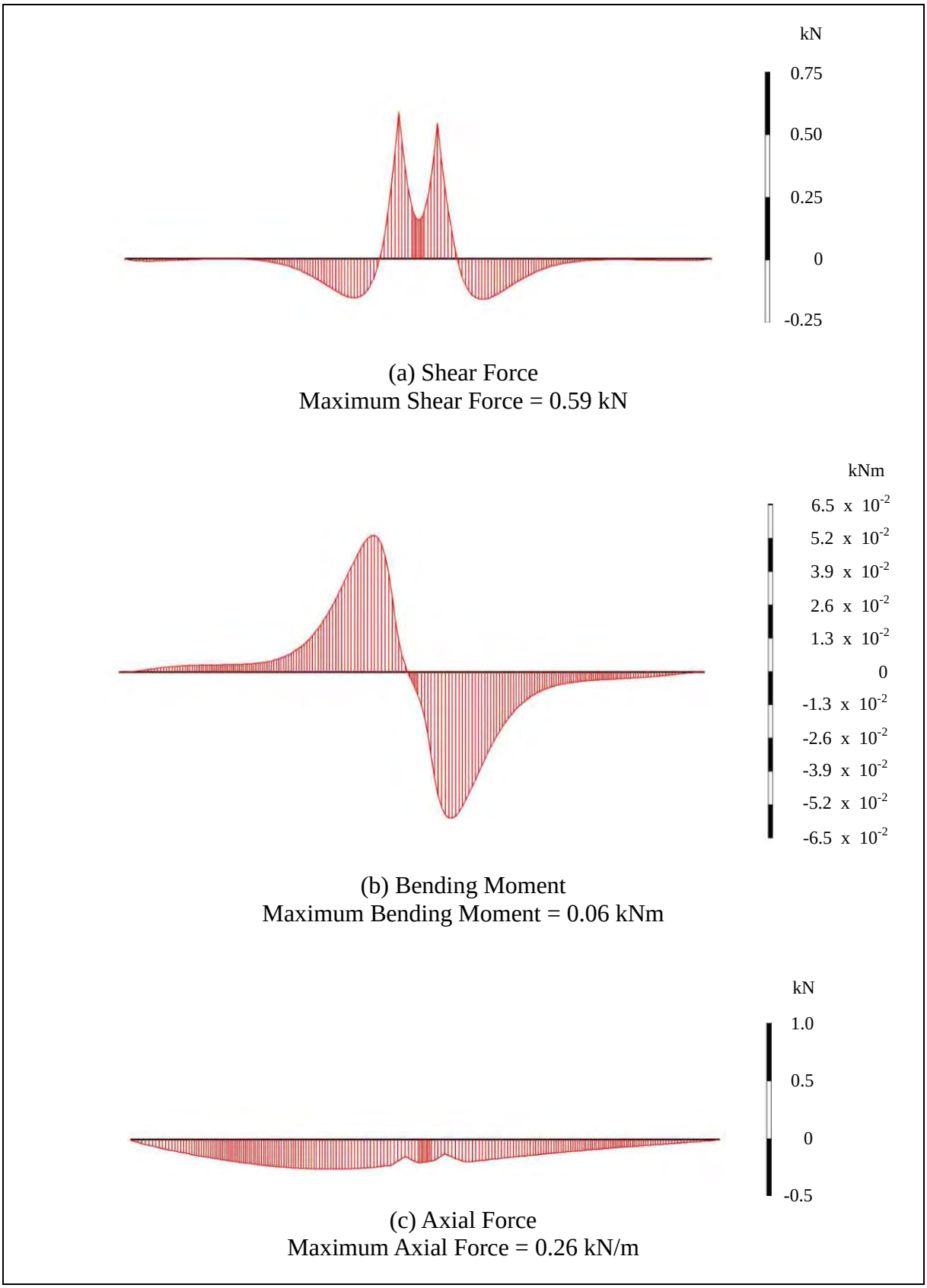

Figure 2.17 Distributions of Shear Force, Bending Moment and Axial Force along the Soil Nail in the 200 mm Zone Numerical Shear Box Test Simulation When δ = 5 mm

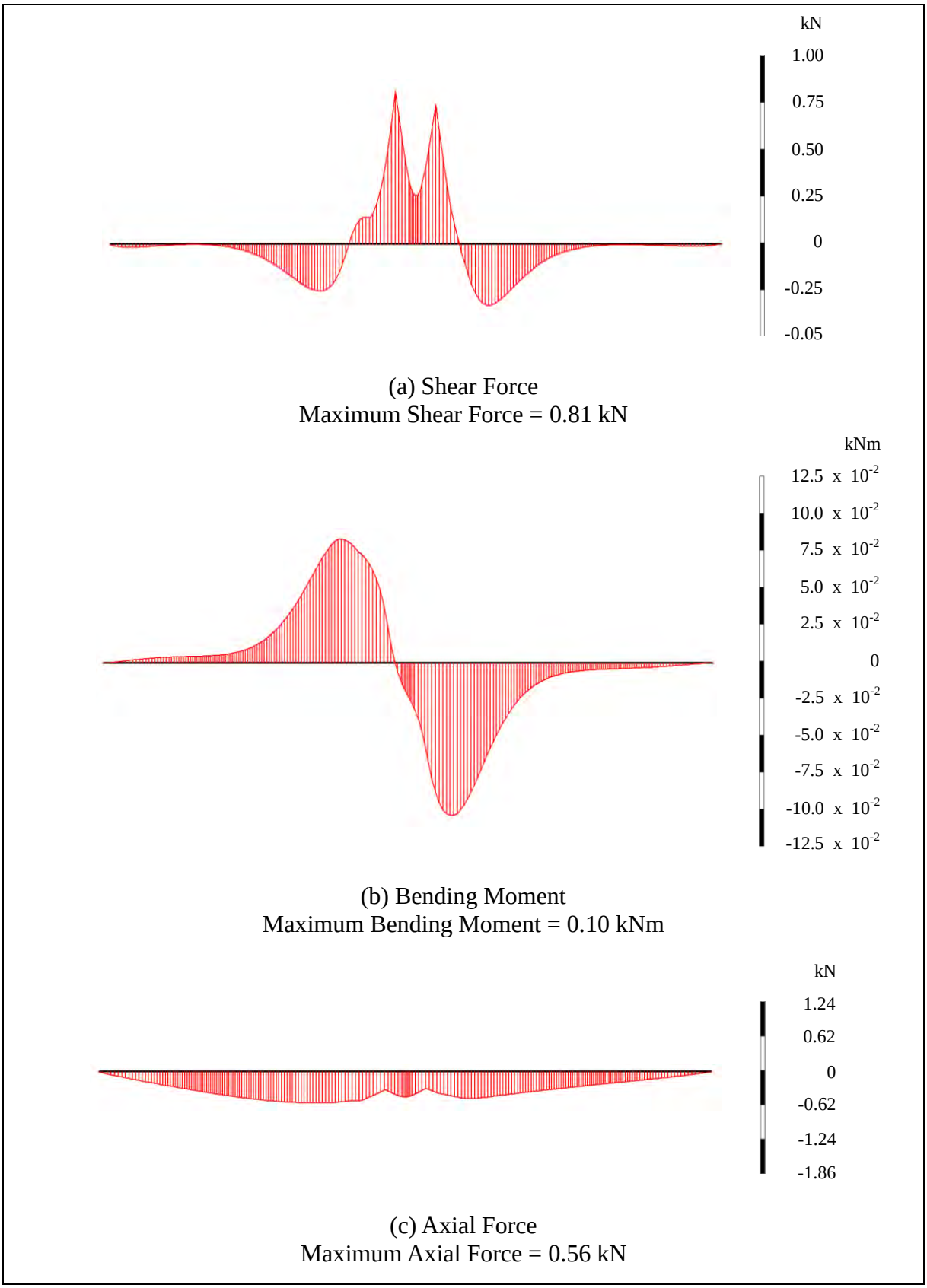

Figure 2.18 Distributions of Shear Force, Bending Moment and Axial Force along the Soil Nail in the 200 mm Zone Numerical Shear Box Test Simulation When δ = 10 mm

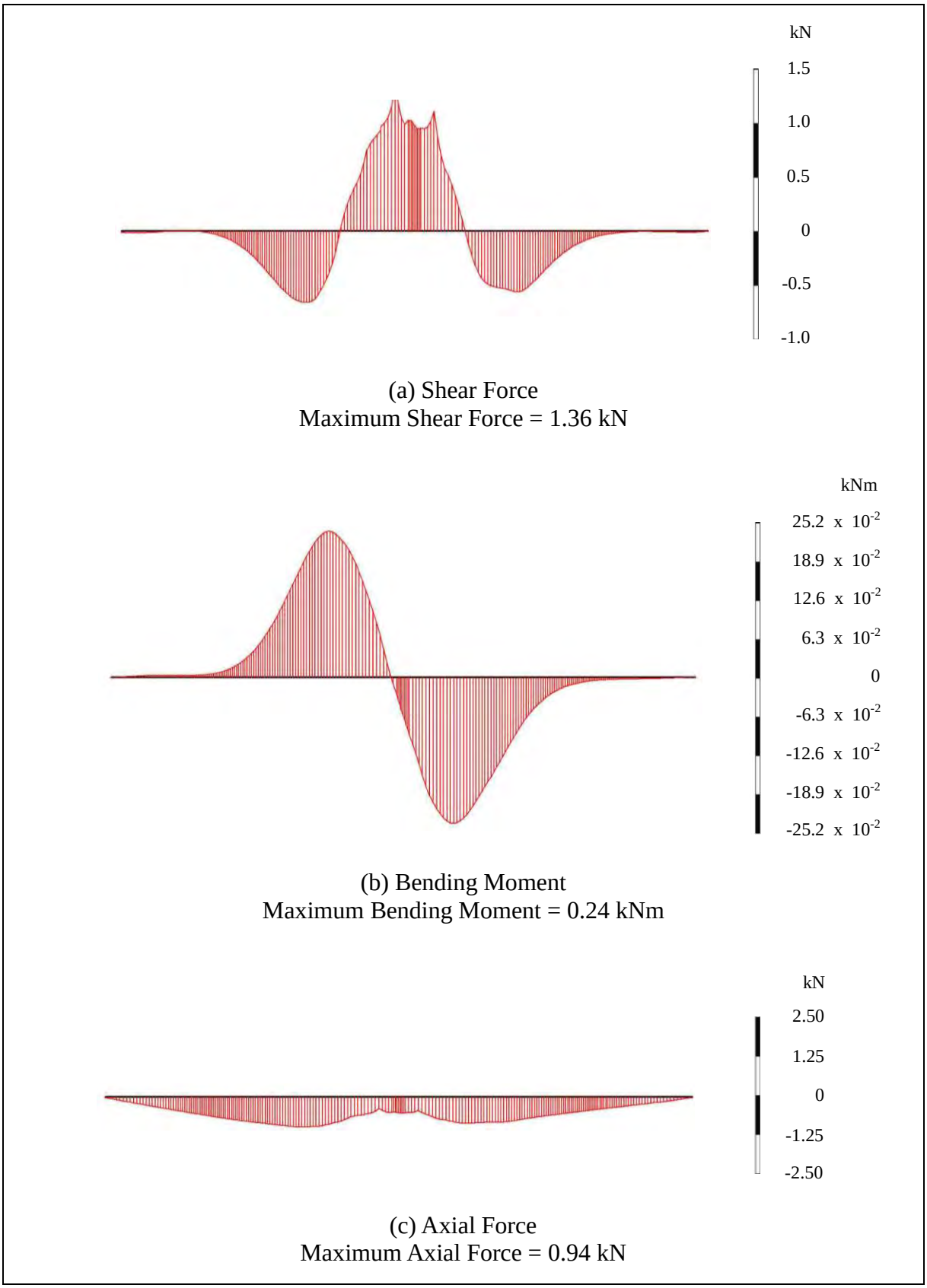

Figure 2.19 Distributions of Shear Force, Bending Moment and Axial Force along the Soil Nail in the 200 mm Zone Numerical Shear Box Test Simulation When δ = 25 mm

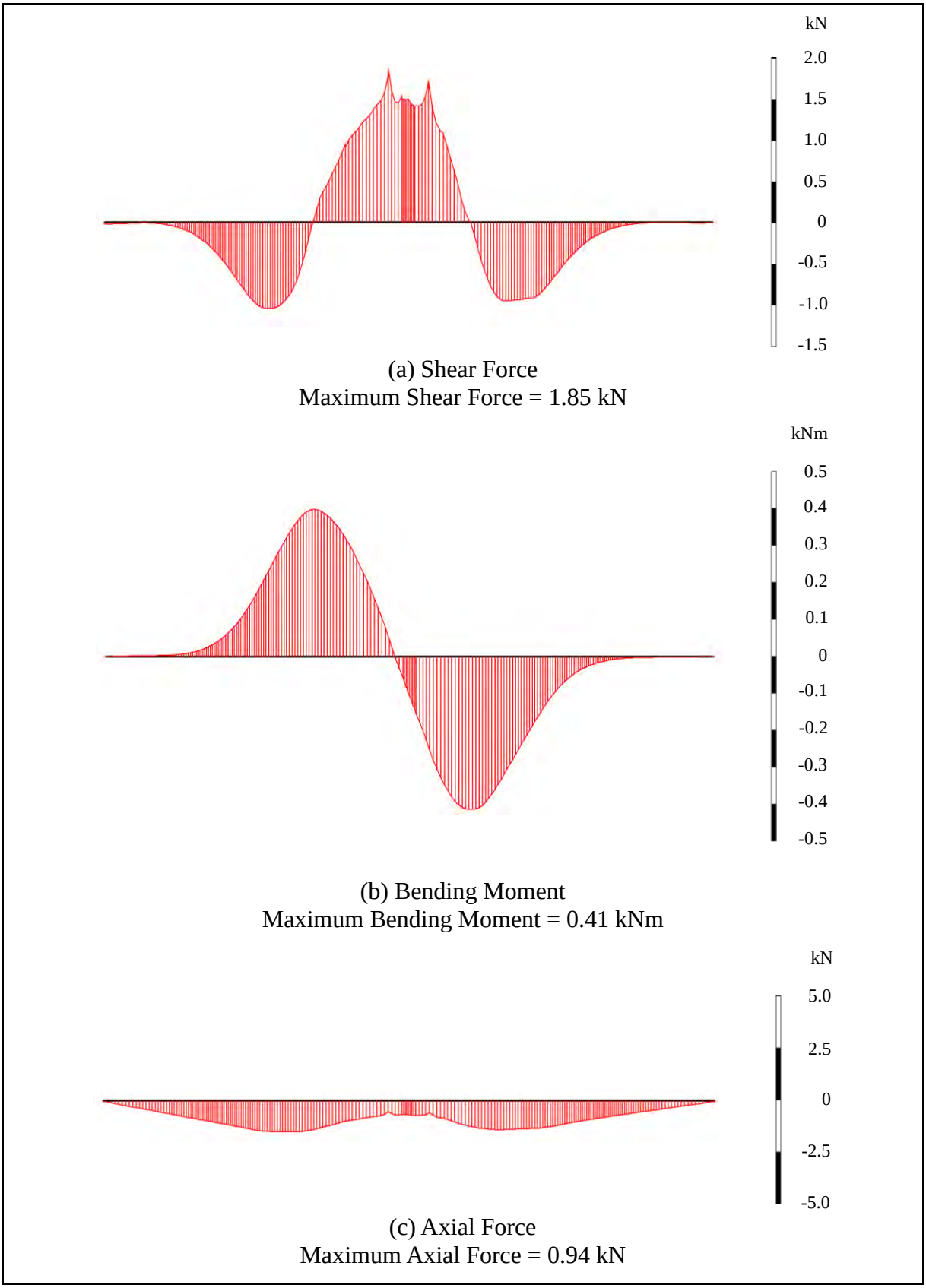

Figure 2.20 Distributions of Shear Force, Bending Moment and Axial Force along the Soil Nail in the 200 mm Zone Numerical Shear Box Test Simulation When δ = 50 mm

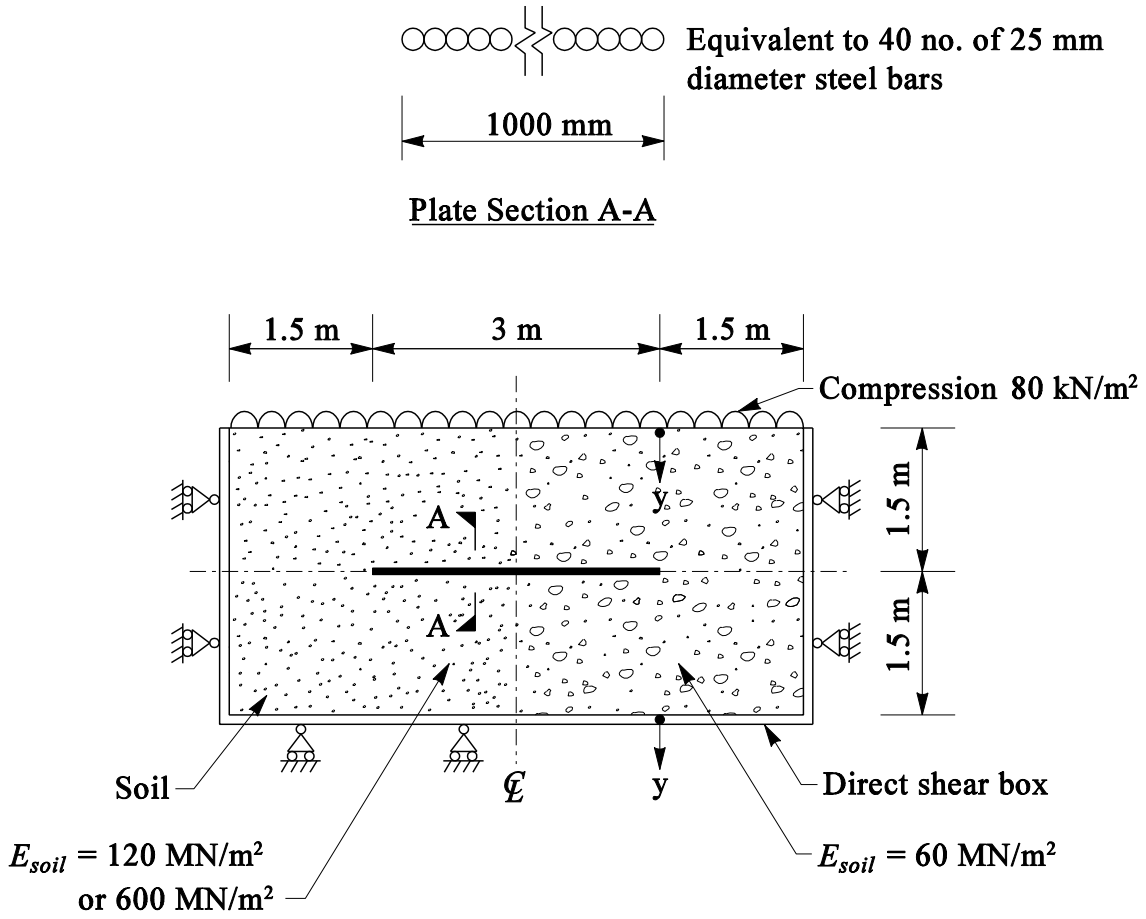

Steel plate size: Equivalent to 40 no. x 25 mm diameter steel bar x 3 m (length)

Steel plate parameters

σ_y = 460 N/mm²
E_{steel} = 205 kN/mm²

Soil sample size: 6 m (length) x 1 m (width) x 3 m (depth)

Soil parameters:

c' = 0 kN/m²
ϕ' = 40°
γ = 16 kN/m³
E_{soil} = 60 MN/m²
ν = 0.4

Prescribed downward boundary shear displacement δ along y-axis = 0, 5, 25, 50 mm at the RHS of the shear box

Figure 2.21 Details of Numerical Direct Shear Box Test Simulation with Soils of Contrast in Stiffness

Similar to those results in numerical direct shear box and zone shear box test simulations, the bending failure mechanism is the critical failure mode if a steel soil nail is subjected to shearing between soils of different stiffness.

2.3 Technical Implications

The results of the numerical simulation have the following technical implications:

(a) When a nail reinforcement is subject to direct shearing, e.g. when the reinforcement is more or less normal to the sliding surface, bending failure is the most critical failure mode. This finding is consistent with the observations in the mode of failure of the nail reinforcement in some soil-nailed slope failures where some steel bars were bent and no shear rupture of the bar was seen.

(b) Because of the high shear ductility of steel reinforcement, which renders the failure mode of a soil-nailed system likely to be ductile, it is generally not necessary to check against bending and shear failure of steel reinforcement in the design. However, if materials other than steel are used for nail reinforcement, their capacity under combined actions of tension, shear and bending should be considered in the design.

3 Conclusions

The behaviour of a steel soil-nail reinforcement subject to shearing has been examined by means of numerical shear box test simulation. The results are consistent with those determined theoretically. The following observations are made:

(a) The mobilisation of axial force, shear force and bending moment in soil nails for a given boundary shear displacement depends on the width of a shear zone. The narrower the shear zone, the higher will be the shear force and bending moment.

(b) The degree of mobilisation of bending moment of a soil nail for a given boundary shear displacement is the highest among the three actions (i.e. axial force, shear force and bending moment). Bending failure will occur first if a steel soil nail is subject to shearing across the nail.

(c) The sharper the contrast in soil stiffness between the two shearing zones, the higher will be the mobilisation of axial force, shear force and bending moment in the soil nails for a given boundary shear displacement.

4 References

GEO (2008). *Guide to Soil Nail Design and Construction (Geoguide 7).* Geotechnical Engineering Office, Hong Kong, 97 p.

Jewell, R.A. & Pedley, M.J. (1992). Analysis for soil reinforcement with bending stiffness. *Journal of Geotechnical Engineering*, ASCE, vol. 118, no. 10, pp 1505-1528.

Pedley, M.J. (1990). The Performance of Soil Reinforcement in Bending and Shear, *PhD thesis*, University of Oxford.

Tan, S.A., Luo, S.Q. & Yong, K.Y. (2000). Simplified models for soil-nail lateral interaction. *Ground Improvement*, Thomas Telford, vol. 4, no. 4, pp 141-152.

GEO PUBLICATIONS AND ORDERING INFORMATION
土力工程處刊物及訂購資料

A selected list of major GEO publications is given in the next page. An up-to-date full list of GEO publications can be found at the CEDD Website http://www.cedd.gov.hk on the Internet under "Publications". Abstracts for the documents can also be found at the same website. Technical Guidance Notes are published on the CEDD Website from time to time to provide updates to GEO publications prior to their next revision.

部份土力工程處的主要刊物目錄刊載於下頁。而詳盡及最新的土力工程處刊物目錄，則登載於土木工程拓展署的互聯網網頁 http://www.cedd.gov.hk 的"刊物"版面之內。刊物的摘要及更新刊物內容的工程技術指引，亦可在這個網址找到。

Copies of GEO publications (except geological maps and other publications which are free of charge) can be purchased either by:

Writing to
Publications Sales Section,
Information Services Department,
Room 402, 4th Floor, Murray Building,
Garden Road, Central, Hong Kong.
Fax: (852) 2598 7482

or

- Calling the Publications Sales Section of Information Services Department (ISD) at (852) 2537 1910
- Visiting the online Government Bookstore at http:// www.bookstore.gov.hk
- Downloading the order form from the ISD website at http://www.isd.gov.hk and submitting the order online or by fax to (852) 2523 7195
- Placing order with ISD by e-mail at puborder@isd.gov.hk

讀者可採用以下方法購買土力工程處刊物(地質圖及免費刊物除外):

書面訂購
香港中環花園道
美利大廈4樓402室
政府新聞處
刊物銷售組
傳真: (852) 2598 7482

或

- 致電政府新聞處刊物銷售小組訂購 (電話：(852) 2537 1910)
- 進入網上「政府書店」選購，網址爲 http://www.bookstore.gov.hk
- 透過政府新聞處的網站 (http://www.isd.gov.hk) 於網上遞交訂購表格，或將表格傳真至刊物銷售小組 (傳真：(852) 2523 7195)
- 以電郵方式訂購 (電郵地址：puborder@isd.gov.hk)

1:100 000, 1:20 000 and 1:5 000 geological maps can be purchased from:

Map Publications Centre/HK,
Survey & Mapping Office, Lands Department,
23th Floor, North Point Government Offices,
333 Java Road, North Point, Hong Kong.
Tel: (852) 2231 3187
Fax: (852) 2116 0774

讀者可於下列地點購買1:100 000、1:20 000及1:5 000地質圖：

香港北角渣華道333號
北角政府合署23樓
地政總署測繪處
電話: (852) 2231 3187
傳真: (852) 2116 0774

Requests for copies of Geological Survey Sheet Reports and other publications which are free of charge should be directed to:

For Geological Survey Sheet Reports which are free of charge:
Chief Geotechnical Engineer/Planning,
(Attn: Hong Kong Geological Survey Section)
Geotechnical Engineering Office,
Civil Engineering and Development Department,
Civil Engineering and Development Building,
101 Princess Margaret Road,
Homantin, Kowloon, Hong Kong.
Tel: (852) 2762 5380
Fax: (852) 2714 0247
E-mail: jsewell@cedd.gov.hk

For other publications which are free of charge:
Chief Geotechnical Engineer/Standards and Testing,
Geotechnical Engineering Office,
Civil Engineering and Development Department,
Civil Engineering and Development Building,
101 Princess Margaret Road,
Homantin, Kowloon, Hong Kong.
Tel: (852) 2762 5346
Fax: (852) 2714 0275
E-mail: thomashui @cedd.gov.hk

如欲索取地質調查報告及其他免費刊物，請致函：

免費地質調查報告:
香港九龍何文田公主道101號
土木工程拓展署大樓
土木工程拓展署
土力工程處
規劃部總土力工程師
(請交:香港地質調查組)
電話: (852) 2762 5380
傳真: (852) 2714 0247
電子郵件: jsewell@cedd.gov.hk

其他免費刊物:
香港九龍何文田公主道101號
土木工程拓展署大樓
土木工程拓展署
土力工程處
標準及測試部總土力工程師
電話: (852) 2762 5346
傳真: (852) 2714 0275
電子郵件: thomashui@cedd.gov.hk

Table of Contents
Table of Contents
Table of Contents

MAJOR GEOTECHNICAL ENGINEERING OFFICE PUBLICATIONS
土力工程處之主要刊物

GEOTECHNICAL MANUALS

Geotechnical Manual for Slopes, 2nd Edition (1984), 302 p. (English Version), (Reprinted, 2011).

斜坡岩土工程手冊(1998)，308頁(1984年英文版的中文譯本)。

Highway Slope Manual (2000), 114 p.

GEOGUIDES

Geoguide 1	Guide to Retaining Wall Design, 2nd Edition (1993), 258 p. (Reprinted, 2007).
Geoguide 2	Guide to Site Investigation (1987), 359 p. (Reprinted, 2000).
Geoguide 3	Guide to Rock and Soil Descriptions (1988), 186 p. (Reprinted, 2000).
Geoguide 4	Guide to Cavern Engineering (1992), 148 p. (Reprinted, 1998).
Geoguide 5	Guide to Slope Maintenance, 3rd Edition (2003), 132 p. (English Version).
岩土指南第五冊	斜坡維修指南，第三版(2003)，120頁(中文版)。
Geoguide 6	Guide to Reinforced Fill Structure and Slope Design (2002), 236 p.
Geoguide 7	Guide to Soil Nail Design and Construction (2008), 97 p.

GEOSPECS

Geospec 1	Model Specification for Prestressed Ground Anchors, 2nd Edition (1989), 164 p. (Reprinted, 1997).
Geospec 3	Model Specification for Soil Testing (2001), 340 p.

GEO PUBLICATIONS

GCO Publication No. 1/90	Review of Design Methods for Excavations (1990), 187 p. (Reprinted, 2002).
GEO Publication No. 1/93	Review of Granular and Geotextile Filters (1993), 141 p.
GEO Publication No. 1/2006	Foundation Design and Construction (2006), 376 p.
GEO Publication No. 1/2007	Engineering Geological Practice in Hong Kong (2007), 278 p.
GEO Publication No. 1/2009	Prescriptive Measures for Man-Made Slopes and Retaining Walls (2009), 76 p.
GEO Publication No. 1/2011	Technical Guidelines on Landscape Treatment for Slopes (2011), 217 p.

GEOLOGICAL PUBLICATIONS

The Quaternary Geology of Hong Kong, by J.A. Fyfe, R. Shaw, S.D.G. Campbell, K.W. Lai & P.A. Kirk (2000), 210 p. plus 6 maps.

The Pre-Quaternary Geology of Hong Kong, by R.J. Sewell, S.D.G. Campbell, C.J.N. Fletcher, K.W. Lai & P.A. Kirk (2000), 181 p. plus 4 maps.

TECHNICAL GUIDANCE NOTES

TGN 1	Technical Guidance Documents